Neuraminidase 1–mediated desialylation of the mucin 1 ectodomain releases a decoy receptor that protects against *Pseudomonas aeruginosa* lung infection

Received for publication, September 26, 2018, and in revised form, November 13, 2018 Published, Papers in Press, November 14, 2018, DOI 10.1074/jbc.RA118.006022

Erik P. Lillehoj[‡1], Wei Guang[‡], Sang W. Hyun[§¶], Anguo Liu[§¶], Nicolas Hegerle[§‖], Raphael Simon[§‖], Alan S. Cross[§‖], Hideharu Ishida[**], Irina G. Luzina[§¶], Sergei P. Atamas[§¶], and Simeon E. Goldblum[§¶‡‡]

From the Departments of [‡]Pediatrics, [§]Medicine, and [‡‡]Pathology and [‖]Institute for Global Health, University of Maryland School of Medicine, Baltimore, Maryland 20201, [¶]U.S. Department of Veterans Affairs, Veterans Affairs Medical Center, Baltimore, Maryland 20201, and [**]Department of Applied Bio-organic Chemistry, Gifu University, Gifu 501-1193 Japan

Edited by Gerald W. Hart

Pseudomonas aeruginosa **(Pa) expresses an adhesin, flagellin, that engages the mucin 1 (MUC1) ectodomain (ED) expressed on airway epithelia, increasing association of MUC1-ED with neuraminidase 1 (NEU1) and MUC1-ED desialylation. The MUC1-ED desialylation unmasks both cryptic binding sites for Pa and a protease recognition site, permitting its proteolytic release as a hyperadhesive decoy receptor for Pa. We found here that intranasal administration of Pa strain K (PAK) to BALB/c mice increases MUC1-ED shedding into the bronchoalveolar compartment. MUC1-ED levels increased as early as 12 h, peaked at 24–48 h with a 7.8-fold increase, and decreased by 72 h. The a-type flagellin–expressing PAK strain and the b-type flagellin–expressing PAO1 strain stimulated comparable levels of MUC1-ED shedding. A flagellin-deficient PAK mutant provoked dramatically reduced MUC1-ED shedding compared with the WT strain, and purified flagellin recapitulated the WT effect. In lung tissues, Pa increased association of NEU1 and protective protein/cathepsin A with MUC1-ED in reciprocal co-immunoprecipitation assays and stimulated MUC1-ED desialylation. NEU1-selective sialidase inhibition protected against Pa-induced MUC1-ED desialylation and shedding. In Pa-challenged mice, MUC1-ED–enriched bronchoalveolar lavage fluid (BALF) inhibited flagellin binding and Pa adhesion to human airway epithelia by up to 44% and flagellin-driven motility by >30%. Finally, Pa co-administration with recombinant human MUC1-ED dramatically diminished lung and BALF bacterial burden, proinflammatory cytokine levels, and pulmonary leukostasis and increased 5-day survival from 0% to 75%. We conclude that Pa flagellin provokes NEU1-mediated airway shedding of MUC1-ED, which functions as a decoy receptor protecting against lethal Pa lung infection.**

Epithelial cells (ECs)[2] lining the airway express multiple receptors that recognize and respond to exogenous danger signals, including bacterial pathogens (1). Host-pathogen interactions include engagement of microbial adhesins with their cognate receptors expressed on the EC surface (2). Such bacterial adhesion to ECs is often a prerequisite to establishment of invasive infection (3). *Pseudomonas aeruginosa* (Pa) is a Gram-negative, flagellated, opportunistic human pathogen that colonizes and/or infects debilitated and immunocompromised patients (4). One Pa adhesin, flagellin, the structural protein of the flagellar filament (5), contributes to its virulence through increased motility, adhesion, and invasion (3), and inflammation through activation of Toll-like receptor (TLR) 5 (6). Pa flagellin also engages the membrane-tethered mucin, MUC1 (7), and this receptor-ligand interaction is coupled to intracellular signaling (8).

MUC1 is a noncovalently associated complex comprised of an NH_2-terminal, heavily sialylated MUC1-ED coupled to a C-terminal MUC1 cytoplasmic domain (MUC1-CD) (9, 10). The MUC1-ED contains a variable number of 20–amino acid (aa) tandem repeats and a Gly-Ser protease recognition site 58 aa upstream of the transmembrane domain, within the proximal, extracellular, juxtamembranous region. The MUC1-ED exhibits a β-turn helix resulting from its high proline content (11). This extended, rodlike conformation allows the MUC1-ED to protrude higher above the EC surface than other membrane-associated proteins, where it is strategically positioned to interact with flagellin-expressing Pa in the airway lumen. The MUC1-ED is up to 90% carbohydrate, almost entirely through >500 predicted *O*-linked glycosylation sites within its tandem repeats (12). Approximately 80% of these *O*-glycan chains ter-

This work was supported by Maryland Technology Development Corporation Grant 0117-005 (to E. P. L.), U.S. Department of Veterans Affairs Grant I01BX002352 (to S. E. G.), and National Institutes of Health Grants AI-110627 (to R. S.), HL-086933 (to A. S. C.), and HL-126897 (to S. P. A.). The authors declare that they have no conflicts of interest with the contents of this article. The content is solely the responsibility of the authors and does not necessarily represent the official views of the National Institutes of Health.

This article contains Figs. S1–S4 and Table S1.

[1] To whom correspondence should be addressed. Tel.: 410-706-3872; Fax: 410-706-0020; E-mail: elillehoj@som.umaryland.edu.

[2] The abbreviations used are: EC, epithelial cell; 4-MU-NANA, 2′-(4-methylumbelliferyl)-α-D-*N*-acetylneuraminic acid; C9-BA-DANA, C9-butyl-amide-2-deoxy-2,3-dehydro-*N*-acetylneuraminic acid; aa, amino acid; Ab, antibody; Ad, adenovirus; BALF, bronchoalveolar lavage fluid; BW, body weight; CD, cytoplasmic domain; CFUs, colony forming units; DANA, 2-deoxy-2,3-dehydro-*N*-acetylneuraminic acid; ED, ectodomain; EGFR, epidermal growth factor receptor; Gal, galactose; i.n., intranasal; i.t., intratracheal; KC, keratinocyte chemoattractant; LB, Luria-Bertani; LPS, lipopolysaccharide; m.o.i., multiplicity of infection; ODN, oligodeoxynucleotide; Pa, *Pseudomonas aeruginosa*; PAK, Pa strain K; PBS-T, PBS containing 0.05% Tween 20; PNA, peanut agglutinin; qRT-PCR, quantitative RT-PCR; STm, *Salmonella enterica* serovar Typhimurium; TNF, tumor necrosis factor.

minate with sialic acid residues (13). There also are five predicted *N*-linked glycosylation sites within the juxtamembranous region (9, 10). Pulse-chase studies have established that MUC1 is initially expressed on the cell surface as an incompletely sialylated glycoform that is subsequently sialylated through several rounds of internalization and recycling back to the surface (14). The relatively short, 72-aa MUC1 cytoplasmic domain contains binding sites for multiple cytosolic signaling molecules, including c-Src (15), epidermal growth factor receptor (EGFR) (16), and γ-catenin (17).

Neuraminidase (NEU)1 has historically been studied in the context of its indispensable role in glycan catabolism (18). We previously established NEU1 as the predominant sialidase expressed in human airway ECs, for which MUC1 is a NEU1 substrate (19, 20). Moreover, in these same cells, Pa-expressed flagellin engages the MUC1-ED to rapidly increase its association with preformed pools of NEU1 and its intracellular chaperone and transport protein, protective protein/cathepsin A (PPCA) (20). NEU1, in turn, desialylates the MUC1-ED, rendering it hyperadhesive for Pa and its flagella. NEU1-mediated desialylation of the MUC1-ED also unmasks the Gly-Ser protease recognition site to permit its proteolytic release from the EC surface into the airway lumen. The shed hyperadhesive MUC1-ED disrupts adhesion of flagellin-expressing Pa to airway ECs. In these same studies, NEU1 overexpression in TLR5-expressing cells failed to desialylate TLR5 or to increase its adhesiveness for Pa. However, these studies were performed exclusively in cultured human airway ECs. Using an intact, physiologically relevant, *in vivo* murine model of Pa pneumonia, we asked whether Pa-derived flagellin might stimulate NEU1-dependent MUC1-ED desialylation to release a hyperadhesive decoy receptor that provides a novel, protective host response to Pa lung infection.

Results

Murine pulmonary responses to Pseudomonas aeruginosa challenge

BALB/c mice were challenged intranasally (i.n.) with Pa strain K (PAK), its flagellin-deficient PAK/fliC^{-} isogenic mutant, Pa strain PAO1, its NEU-deficient PAO1/NanPs^{-} isogenic mutant, or clinical Pa isolates obtained from patients diagnosed with pneumonia, at either sublethal (1.0×10^5 colony-forming units (CFUs)/mouse) or lethal (2.0×10^7 CFUs/mouse) inocula. Pa CFUs in lung tissues and bronchoalveolar lavage fluid (BALF) increased at 6 h following challenge with PAK at 1.0×10^5 CFUs/mouse, after which Pa lung burden peaked at 12 h, whereas BALF CFUs peaked at 24 h (Fig. S1*A*). CFUs in both lung tissue and BALF decreased by 48 h. In these same Pa-challenged mice, BALF levels of the proinflammatory cytokine tumor necrosis factor (TNF)-α and the chemokine keratinocyte chemoattractant (KC) increased as early as 6 h, continuing to increase over the 48-h study period (Fig. S1*B*). Lung myeloperoxidase (MPO) activity, a biochemical marker of neutrophil recruitment, increased at 6 h, peaked at 12 h, after which it was sustained through 48 h (Fig. S1*C*). Histological studies of stained lung sections harvested 24 h after Pa challenge revealed intense neutrophil infiltration of lung parenchyma compared with lung sections from the simultaneous PBS controls (Fig. S1*D*). The 5-day survival of mice challenged with 1.0×10^5 CFUs/mouse was 100%, whereas for those challenged with 2.0×10^7 CFUs/mouse it was 0% (Fig. S1*E*). This *in vivo* model of acute Pa lung infection and the airway responses to Pa were used to study MUC1-ED shedding as a Pa-targeting, host defense mechanism.

Flagellin-expressing Pa increases MUC1-ED shedding within murine airways

The MUC1-ED is reportedly shed from the surface of extrapulmonary epithelia (21–24). In cultured human gastric ECs, *Helicobacter pylori*–induced MUC1-ED shedding constitutes an important component of the host response to limit bacterial infection (24). We asked whether the MUC1-ED might be shed from airway epithelia *in vivo*, and if so, whether Pa might stimulate shedding. Mice were administered i.n. with a WT PAK challenge of 1.0×10^5 CFUs/mouse, an equivalent challenge of the flagellin-deficient isogenic mutant, PAK/fliC^{-}, or an equivalent volume of the PBS vehicle alone. At increasing times postchallenge, BALF was collected and MUC1-ED quantified by enzyme-linked immunosorbent assay (ELISA) and normalized to total BALF protein. In the BALF of WT PAK-challenged mice, MUC1-ED levels increased as early as 12 h compared with the simultaneous controls, with further time-dependent increases through 24 h, after which it plateaued and remained elevated through 48 h, and was decreasing at 72 h (Fig. 1*A*). In BALF of mice challenged with the flagellin-deficient PAK/fliC^{-} mutant, MUC1-ED levels modestly increased at 24 h compared with the simultaneous controls, but were dramatically reduced at 24 h and 48 h postchallenge compared with WT PAK-challenged mice (Fig. 1*A*). In contrast, MUC1-ED levels in the BALF of simultaneous PBS-administered controls remained relatively unchanged over the 72-h study period. At 24 h, BALF MUC1-ED levels in Pa-challenged mice were increased 7.8-fold compared with levels measured in the PBS-administered controls. In other experiments, mice were administered i.n. with increasing inocula of PAK and, after 24 h, BALFs collected and MUC1-ED levels assayed and normalized. Pa inocula of $\geq 5.0 \times 10^3$ CFUs/mouse increased MUC1-ED levels in BALF, without further increments in response to increasing Pa inocula (Fig. 1*B*). Mice challenged i.n. with PAK/fliC^{-} displayed dramatically reduced levels of MUC1-ED shedding compared with WT PAK (Fig. 1, *A* and *C*). However, the PAK/fliC^{-} strain still increased MUC1-ED shedding compared with the PBS control, indicating that one or more Pa constituent(s) other than flagellin might also be operative. Purified Pa lipopolysaccharide (LPS), Pam_3Cys-Ser-(Lys)4 as a bacterial lipoprotein mimetic, and CpG oligodeoxynucleotide (ODN) 1826 as a bacterial DNA mimetic, all failed to increase MUC1-ED shedding (Fig. 1*C*). Each Pa strain expresses one of two types of flagellin, a-type (FlaA) or b-type (FlaB) (25). The FlaA-expressing PAK strain dramatically increased MUC1-ED shedding (Fig. 1, *A*–*C*). We asked whether PAO1, a FlaB-expressing strain, might also induce MUC1-ED shedding. Equivalent inocula of PAK and PAO1 provoked comparable levels of MUC1-ED shedding, as did equivalent inocula of five clinical strains of Pa isolated from pneumonia patients, three express-

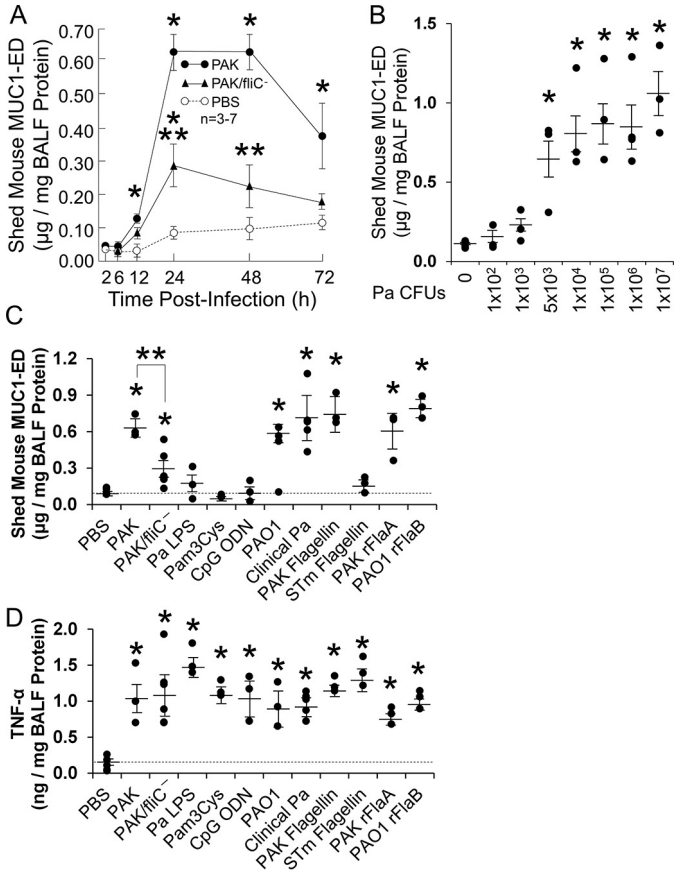

Figure 1. Flagellin-expressing Pa induces MUC1-ED shedding *in vivo*. *A*, BALB/c mice were administered i.n. with 1.0×10^5 CFUs/mouse of WT PAK or the flagellin-deficient PAK/fliC$^-$ mutant, or the PBS vehicle. At increasing times postinfection, BALF was collected, and MUC1-ED levels quantified by ELISA and normalized to BALF protein. *B*, at 24 h postinfection with increasing inocula of WT PAK, MUC1-ED levels in BALF were quantified and normalized to BALF protein. *C* and *D*, BALB/c mice were infected i.n. with 1.0×10^5 CFUs of the indicated strains of Pa, or were administered i.n. with PBS, 10 ng of Pa or STm flagellins, 10 ng of Pa rFlaA or rFlaB expressed in *E. coli*, 100 ng of Pa LPS, 10 μg of Pam_3Cys-Ser-(Lys)4, or 10 μg of CpG ODN 1826. At 24 h postinfection/administration, MUC1-ED levels (*C*) and TNFα levels (*D*) in BALF were quantified and normalized to BALF protein. *C* and *D*, the *dashed lines* indicate the levels of MUC1-ED shedding and TNFα in mice administered with PBS for comparison with the other experimental groups. *Error bars* represent mean ± S.E. values ($n = 3$–7). *, increased MUC1-ED/TNFα levels compared with uninfected or PBS controls at $p < 0.05$. **, decreased MUC1-ED levels following infection with the flagellin-deficient PAK/fliC$^-$ strain compared with flagellin-expressing WT PAK at $p < 0.05$. The results are representative of three independent experiments.

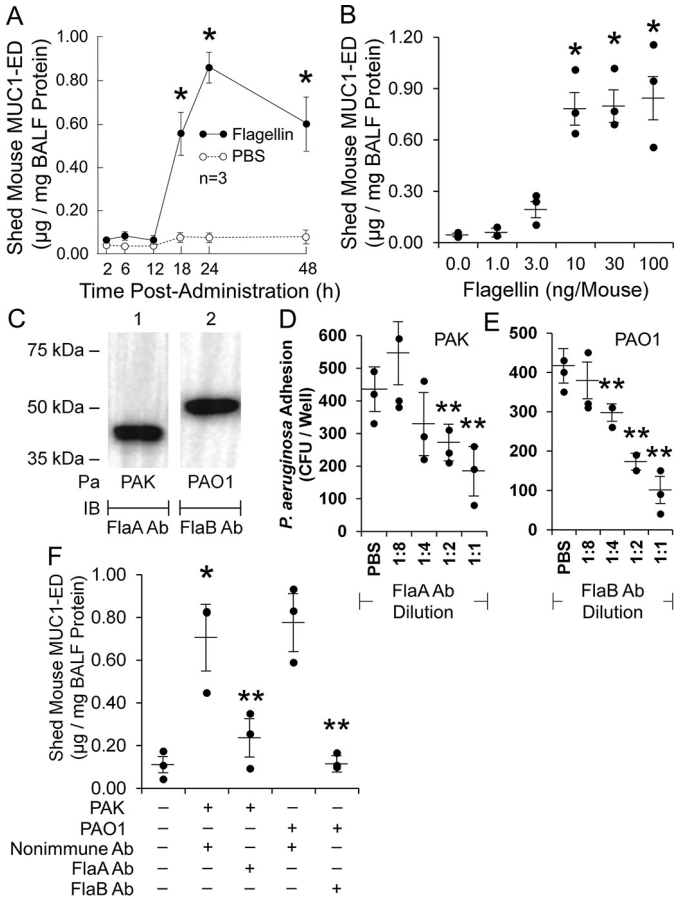

Figure 2. Purified Pa flagellin recapitulates Pa-provoked MUC1-ED shedding *in vivo*. *A*, BALB/c mice were administered i.n. with 10 ng/mouse of PAK flagellin or the PBS vehicle. At increasing times posttreatment, MUC1-ED levels in BALF were quantified and normalized to BALF protein. *B*, mice were administered increasing doses of PAK flagellin. At 24 h posttreatment, MUC1-ED levels in BALF were quantified and normalized to BALF protein. *C*, lysates of PAK and PAO1 were processed for flagellin immunoblotting using mouse anti-FlaA (*lane 1*) or anti-FlaB (*lane 2*) polyclonal antisera. Molecular masses in kDa are indicated on the left. *D* and *E*, PAK (*D*) or PAO1 (*E*) (1.0×10^7 CFUs) were incubated for 30 min at 4 °C with undiluted or decreasing dilutions of 100 μl of anti-FlaA (*D*) or anti-FlaB (*E*) antisera or the PBS control. The bacteria were washed and processed for adhesion to Ad-NEU1–infected (multiplicity of infection (m.o.i.) = 100) A549 cells. *F*, PAK (1.0×10^5 CFU) was preincubated with 10 μl of anti-FlaA antiserum or nonimmune mouse serum, and PAO1 (1.0×10^5 CFUs) was preincubated with 10 μl of anti-FlaB antiserum or nonimmune mouse serum for 30 min at 4 °C and washed. BALB/c mice were infected i.n. with the bacteria or administered the PBS vehicle. At 24 h postinfection, MUC1-ED levels in BALF were quantified and normalized to BALF protein. *Error bars* represent the mean ± S.E. values ($n = 3$). *, increased MUC1-ED levels compared with (*A* and *B*) PBS controls or (*F*) nonimmune mouse serum at $p < 0.05$. **, (*E*) decreased Pa adhesion compared with PBS controls, or (*F*) decreased MUC1-ED levels compared with nonimmune Ab, at $p < 0.05$. The results are representative of three independent experiments.

ing FlaA and two expressing FlaB (Fig. 1*C*). Further, FlaA purified from PAK, but not flagellin purified from *Salmonella enterica* serovar Typhimurium (STm), reconstituted the viable Pa effect (Fig. 1*C*). That STm flagellin failed to provoke MUC1-ED shedding excluded participation of TLR5. Finally, *Escherichia coli*–expressed recombinant (r) FlaA and rFlaB, cloned from PAK and PAO1, respectively, also stimulated MUC1-ED shedding (Fig. 1*C*). To establish *in vivo* biological activities, each reagent was administered and shown to elevate BALF TNFα levels (Fig. 1*D*). Our results likely underestimate the levels of shed MUC1-ED within the alveolar lining fluid (26) and the mucus blanket that covers the airway epithelium (27). Further, a dilutional effect is intrinsic to the BAL procedure (28), and some loss of protein is anticipated during MUC1-ED preparation (20).

Pa-derived flagellin increases MUC1-ED shedding within the murine airway

To further establish that purified, LPS-free flagellin could recapitulate the Pa effect, mice were administered a fixed dose of PAK-expressed flagellin, and at increasing times postchallenge, BALF was collected and MUC1-ED levels quantified. The kinetics for flagellin-induced MUC1-ED shedding were similar to those seen after viable WT PAK challenge with minor differences. Pa-induced shedding was first detected at 12 h (Fig. 1*A*), whereas flagellin-induced shedding was not apparent until 18 h (Fig. 2*A*). Further, Pa-induced shedding began to

decrease by 72 h (Fig. 1*A*), whereas that seen after flagellin administration decreased as early as 48 h (Fig. 2*A*). Flagellin at doses ≥10 ng/mouse, like viable Pa, dose-dependently increased MUC1-ED levels in BALF (Fig. 2*B*). Given that Pa expresses a single, polar flagellum (5), and based on an estimated 3.0×10^4 flagellin monomers per flagellar filament (29), Pa inocula of 5.0×10^3 CFUs/mouse that induce MUC1-ED shedding (Fig. 1*B*) are estimated to express $\sim 2.5 \times 10^{-8}$ ng of flagellin. Differences between Pa- and flagellin-induced MUC1-ED shedding might be explained, in part, through an imperfect correlation between Pa inoculum size (in CFUs/mouse) and Pa flagellin expression (in ng/mouse), differences in intra-airway half-life of Pa-associated *versus* free, soluble flagellin, and/or diminished flagellin bioactivity during its purification.

We next asked whether anti-flagellin antisera might block flagellin-induced increases in MUC1-ED shedding. To establish the specificity of our mouse anti-flagellin antisera, immunoblot analysis using whole cell extracts of PAK and PAO1 revealed immunoreactive bands corresponding to the anticipated 45.0 kDa FlaA and 53.0 kDa FlaB flagellins, respectively (25) (Fig. 2*C*). Further, incubation of PAK and PAO1 with decreasing dilutions of anti-FlaA and anti-FlaB antisera, respectively, dose-dependently blocked Pa adhesion to human airway ECs infected with adenovirus-encoding NEU1 (Ad-NEU1) (Fig. 2, *D* and *E*). These same antisera dramatically reduced Pa-stimulated MUC1-ED shedding in mouse lungs compared with bacteria incubated with a nonimmune mouse serum (Fig. 2*F*). These combined data indicate that 1) flagellin is absolutely required and sufficient to induce MUC1-ED shedding *in vivo*, 2) flagellin-induced MUC1-ED shedding is dose- and time-dependent, and 3) both FlaA and FlaB flagellins provoke comparable MUC1-ED shedding.

Effect of Pa infection on NEU1 and PPCA expression and sialidase activity in murine lung

The predominant sialidase in human airway epithelia, NEU1, explains >70% of total EC sialidase activity for the 2′-(4-methylumbelliferyl)-α-D-*N*-acetylneuraminic acid (4-MU-NANA) substrate (19). NEU1 immunostaining of normal human lung tissues localized the sialidase almost exclusively to the superficial epithelium lining the trachea, main stem and segmented bronchi, and alveoli (19), and Pa-induced MUC1-ED shedding from human airway ECs was absolutely NEU1-dependent (20). Further, not only did NEU1 overexpression increase shedding, but silencing of NEU1 expression (19) and NEU1-selective sialidase inhibition with C9-butyl-amide-2-deoxy-2,3-dehydro-*N*-acetylneuraminic acid (C9-BA-DANA) (30), each dramatically reduced flagellin-induced shedding (20). In these same human airway ECs, flagellin stimulation failed to up-regulate NEU1 mRNA or protein expression or total sialidase activity (20). Because mouse lung contains multiple cell types other than ECs that could potentially respond to Pa and/or flagellin, we harvested lung tissues from Pa-challenged and control mice and measured NEU1 transcript levels by quantitative RT-PCR (qRT-PCR) and NEU1 protein levels by quantitative immunoblotting. No increases in NEU1 mRNA or protein were detected (Fig. S2, *A*, *C*, and *D*). Because NEU1 catalytic activity may be regulated through its chaperone/transport protein, PPCA, the lung tissues were similarly studied for PPCA mRNA and protein. Again, no up-regulation of PPCA mRNA or protein was detected (Fig. S2, *B*, *E*, and *F*). Finally, in these same tissues, no increases in total sialidase activity were found in Pa-challenged mice compared with the PBS controls (Fig. S2*G*). These combined data raised the possibility that preformed pools of NEU1 and/or PPCA might be mobilized in response to the Pa/flagellin stimulus.

Pa increases NEU1/PPCA association with and desialylation of the MUC1-ED in murine lung

We next asked whether flagellin-expressing Pa might increase NEU1/PPCA association with and desialylation of the MUC1-ED in the lungs of Pa-challenged mice. Mice were administered PAK (1.0×10^5 CFUs/mouse) or PBS alone, and after 6 h, lungs were harvested and processed for reciprocal NEU1-MUC1 and PPCA-MUC1 co-immunoprecipitation assays. In the lungs of Pa-challenged mice, MUC1 co-immunoprecipitation of NEU1 increased 2.4-fold (Fig. 3, *A*, *lanes 1* and *2*, and *B*) and NEU1 co-immunoprecipitation of MUC1 increased 4.2-fold (Fig. 3, *A*, *lanes 3* and *4*, and *C*) compared with their respective controls. In these same lungs, MUC1 co-immunoprecipitation of PPCA increased 3.4-fold (Fig. 3, *A*, *lanes 5* and *6*, and *D*) and PPCA co-immunoprecipitation of MUC1 increased 1.8-fold (Fig. 3, *A*, *lanes 7* and *8*, and *E*). Because NEU1 association with its MUC1 substrate was elevated in response to Pa administration, and NEU1-mediated desialylation of the MUC1-ED permits its increased proteolytic release (20), we simultaneously assessed the sialylation state of shed MUC1-ED in the BALF and airway EC-associated MUC1-ED retained in lung tissues using peanut agglutinin (PNA) to selectively recognize desialylated MUC1-ED. To validate the PNA lectin, we showed that PNA recognized asialofetuin but not fetuin (Fig. 3*F*). At 24 h after administration of Pa or the PBS control, BALF and lung tissues were collected and lungs homogenized. The BALFs and lung homogenates were processed for quantitative MUC1-ED immunoblotting (Fig. 3*G*), or incubated with PNA immobilized on agarose beads and the PNA-binding proteins processed for MUC1-ED immunoblotting (Fig. 3, *H–J*). In the BALF of Pa-challenged mice, shed MUC1-ED levels were increased compared with the PBS controls (Fig. 3*G*, *lanes 2 versus 1*), whereas in lung tissues they remained unchanged (Fig. 3*G*, *lanes 4 versus 3*). In the BALF, desialylation of shed MUC1-ED was increased 2.8-fold compared with the simultaneous controls (Fig. 3, *H*, *lanes 2 versus 1*, and *I*), whereas in lung tissues, the MUC1-ED sialylation state remained unchanged (Fig. 3, *H*, *lanes 4 versus* 3, and *J*). Taken together, these data indicate that Pa lung infection does not increase NEU1/PPCA expression or total sialidase activity, but rather, increases the association of NEU1 and PPCA with MUC1, and NEU1-mediated MUC1-ED desialylation plays a permissive role for shedding. Sialylated MUC1-ED, on the other hand, was more resistant to shedding and remained associated with the EC surface.

Participation of NEU1 in Pa-provoked MUC1-ED shedding

Pa administration increased NEU1 and PPCA association with MUC1 (Fig. 3, *A–E*) and augmented MUC1-ED desialyla-

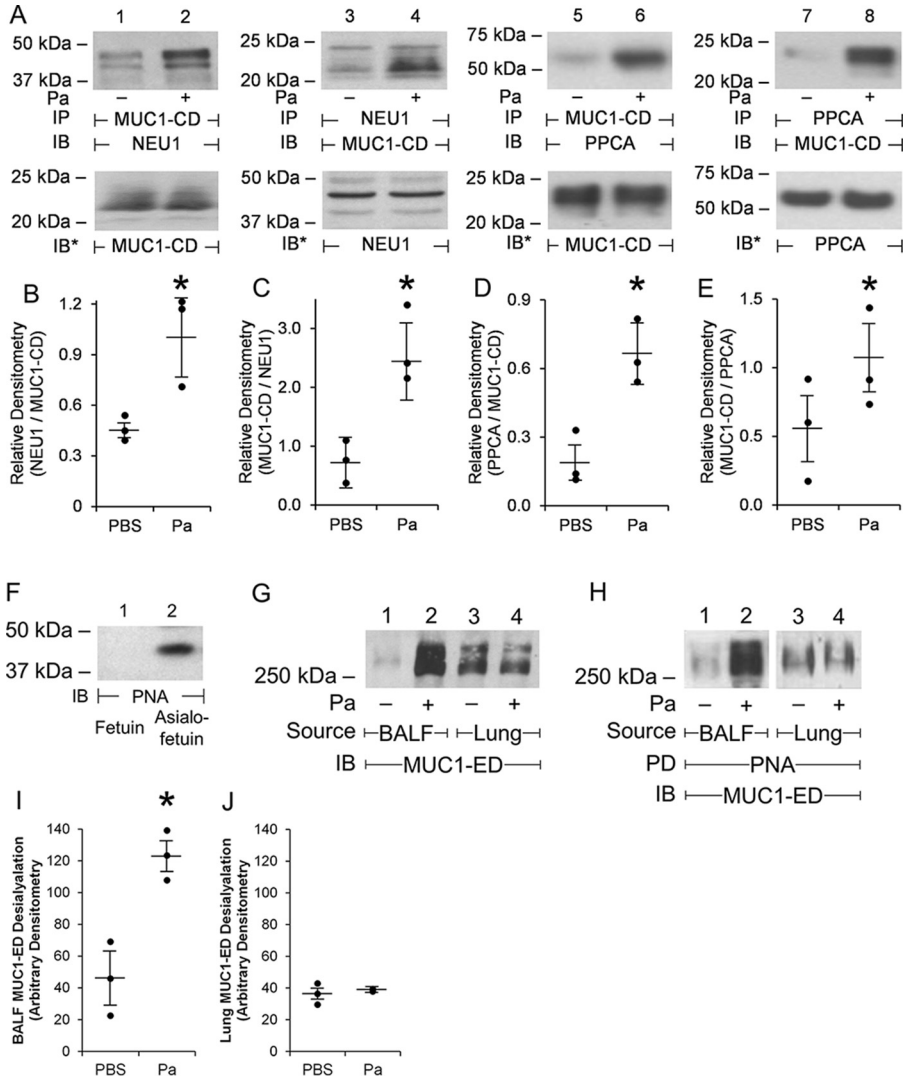

Figure 3. Pa lung infection increases NEU1-MUC1 and PPCA-MUC1 association and MUC1-ED desialylation. *A–E* and *G–J*, BALB/c mice were administered i.n. with 1.0×10^5 CFUs/mouse of PAK or the PBS vehicle. At 24 h postchallenge, BALF and lung tissues were collected, and lungs were homogenized. *A*, lung homogenates were immunoprecipitated with anti-MUC1-CD (*lanes 1*, *2*, *5*, *6*), anti-NEU1 (*lanes 3*, *4*), or anti-PPCA (*lanes 7*, *8*) Abs. The MUC1-CD immunoprecipitates were processed for NEU1 (*lanes 1*, *2*) or PPCA (*lanes 5*, *6*) immunoblotting, and the NEU1 (*lanes 3*, *4*) and PPCA (*lanes 7*, *8*) immunoprecipitates were processed for MUC1-CD immunoblotting (*upper panels*). To control for protein loading and transfer, the immunoblots were stripped and reprobed with the immunoprecipitating Ab (*lower panels*). *B–E*, densitometric analyses of the blots in (*A*). *Error bars* represent mean ± S.E. MUC1-CD, NEU1, or PPCA signal normalized to the immunoprecipitate signal in the same lane on the same stripped and reprobed blot ($n = 3$). *, increased normalized lung NEU1, MUC1-CD, or PPCA signal compared with PBS controls at $p < 0.05$. *F*, to validate PNA selectivity, the negative control, fetuin (*lane 1*), and the positive control, asialofetuin (*lane 2*), 1.0 μg each, were processed for PNA lectin blotting. *G*, BALF (*lanes 1* and *2*) and lung homogenates (*lanes 3* and *4*) from mice administered i.n. with PAK or the PBS vehicle were processed for MUC1-ED immunoblotting. *H*, BALF (*lanes 1* and *2*) and lung homogenates (*lanes 3* and *4*) were incubated with PNA-agarose and the PNA-binding proteins processed for MUC1-ED immunoblotting. *I* and *J*, densitometric analyses of the blots in (*H*). *Error bars* represent mean ± S.E. BALF/lung desialylated MUC1-ED signal ($n = 3$). *, increased BALF MUC1-ED signal compared with PBS controls at $p < 0.05$. (*A* and *F–H*), molecular masses in kDa are indicated on the *left*. *IP*, immunoprecipitate; *IB*, immunoblot; *IB**, immunoblot after stripping. *PD*, pulldown. The results are representative of three independent experiments.

tion (Fig. 3, *H* and *I*). We asked whether Pa-induced MUC1-ED desialylation was mediated through NEU1. Mice were pretreated with increasing concentrations of the NEU1-selective sialidase inhibitor C9-BA-DANA (30), or the broad-spectrum sialidase inhibitor 2-deoxy-2,3-dehydro-*N*-acetylneuraminic acid (DANA) (32, 33), or PBS alone. After 24 h, mice were challenged with PAK and, after 48 h, BALF harvested and MUC1-ED desialylation and levels quantified. NEU1-selective sialidase inhibition with 170 nmol/g body weight of C9-BA-DANA protected against Pa-provoked MUC1-ED desialylation by >80% (Fig. 4, *A* and *B*) and shedding by >50% (Fig. 4*C*). Broad-spectrum sialidase inhibition with an equivalent amount of DANA protected against MUC1-ED desialylation by >85% (Fig. 4, *A* and *B*) and shedding by 65% (Fig. 4*C*). Prior sialidase inhibition with C9-BA-DANA or DANA dramatically reduced the relative abundance of total BALF MUC1-ED (Fig. 4*D*, *lanes 2 versus 1* and *lanes 4 versus 3*). Broad-spectrum sialidase inhibition with 50 nmol/g of DANA provided greater protection against MUC1-ED desialylation and shedding than did an equivalent dose of the NEU1-selective inhibitor, C9-BA-DANA (Fig. 4, *A–C*). It is conceivable that NEUs other than NEU1 contribute to MUC1-ED desialylation.

We next asked whether ectopic overexpression of NEU1 *in vivo* might provoke MUC1-ED desialylation and shedding in

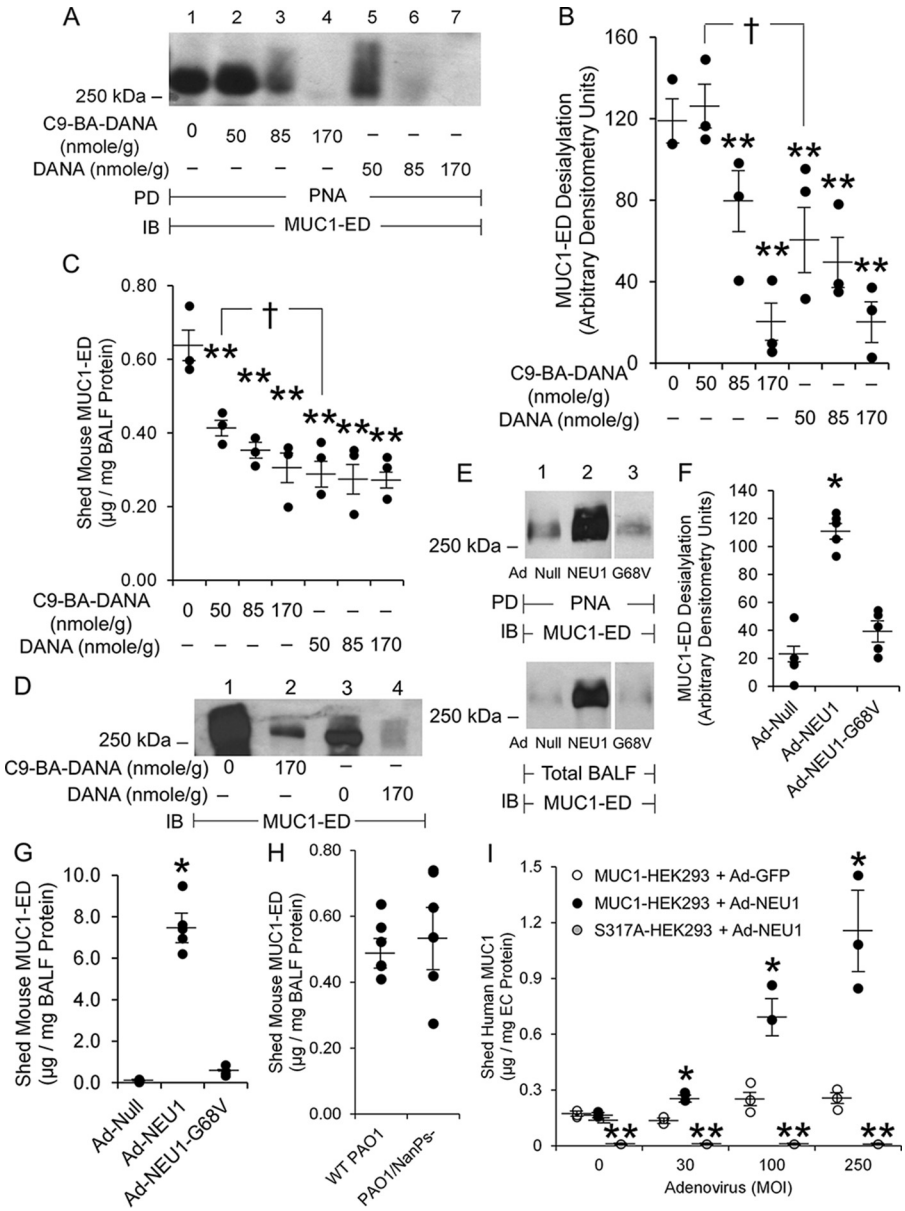

Figure 4. NEU1 is required for maximal Pa-induced MUC1-ED desialylation and shedding. *A–D*, BALB/c mice were administered intraperitoneally with the indicated amounts of C9-BA-DANA, DANA, or the PBS vehicle. At 24 h postadministration, mice were infected i.n. with 1.0×10^5 CFUs/mouse of PAK. At 24 h postinfection, BALF was collected. *A*, BALFs were incubated with PNA-agarose and the PNA-binding proteins processed for MUC1-ED immunoblotting. *B*, densitometric analyses of the blots in (*A*). *B* and *C*, *error bars* represent mean ± S.E. BALF desialylated MUC1-ED signal or shed MUC1-ED levels ($n = 3$). *C*, BALF MUC1-ED levels were quantified by ELISA and normalized to BALF protein. *D*, BALFs were processed for MUC1-ED immunoblotting. **, decreased desialylated MUC1-ED signal or MUC1-ED level compared with PBS control at $p < 0.05$. †, decreased desialylated MUC1-ED signal or MUC1-ED level in mice administered DANA compared with mice administered C9-BA-DANA at $p < 0.05$. *E–G*, BALB/c mice were administered i.t. with Ad-NEU1, Ad-NEU1-G68V, or Ad-Null. At 3 days postinfection, BALF was collected. *E*, BALFs were incubated with PNA-agarose and the PNA-binding proteins processed for MUC1-ED immunoblotting. *F*, densitometric analyses of the blots in (*E*). *G*, BALF MUC1-ED levels were quantified by ELISA and normalized to BALF protein. *F* and *G*, *error bars* represent mean ± S.E. BALF desialylated MUC1-ED signal or MUC1-ED levels ($n = 5$). *, increased desialylated MUC1-ED signal or MUC1-ED level compared with Ad-Null or Ad-NEU1-G68V controls at $p < 0.05$. *A*, *D*, and *E*, Molecular masses in kDa are indicated on the *left*. *H*, BALB/c mice were infected i.n. with 1.0×10^5 CFUs of WT NanPs-expressing PAO1 or the NanPs-deficient PAO1/NanPs$^-$ isogenic mutant. At 24 h postinfection, MUC1-ED levels in BALF were quantified and normalized to BALF protein ($n = 6$). *I*, HEK293 cells were transfected with plasmids encoding for WT MUC1 or the MUC1-ED S317A protease recognition site mutant and incubated for 24 h. The ECs were infected with increasing m.o.i.s of Ad-GFP or Ad-NEU1. After 48 h, shed MUC1-ED levels in cell culture supernatants were quantified by ELISA and normalized to total supernatant protein. *Error bars* represent mean ± S.E. shed MUC1-ED levels ($n = 3$). *, increased MUC1-ED levels *versus* Ad-GFP-infected MUC1-HEK293 cells at $p < 0.05$. **, decreased MUC1-ED levels *versus* Ad-NEU1-infected MUC1-HEK293 cells at $p < 0.05$. The results are representative of three independent experiments. *IB*, immunoblot; *PD*, pulldown.

the absence of a Pa stimulus. Mice infected intratracheally (i.t.) with an adenovirus encoding human NEU1 (Ad-NEU1), but not Ad-encoding the empty vector (Ad-Null), exhibited elevated expression of human NEU1 mRNA in lung homogenates that was maximal on day 3 postinfection, with time-dependent decreases on days 7 and 14 (34). In the BALF of mice infected i.t. with Ad-NEU1, desialylation of shed MUC1-ED was increased 5.5-fold at 3 days postinfection (Fig. 4, *E*, *lanes 2 versus 1*, and *F*), and MUC1-ED shedding was dramatically increased 148-fold (Fig. 4*G*), each compared with the simultaneous Ad-Null controls. Similar increases in MUC1-ED desialylation (Fig. 4, *E* and *F*) and shedding (Fig. 4*G*) were seen in BALF of mice infected i.t.

with Ad-NEU1 compared with Ad-encoding catalytically inactive NEU1 containing a Gly^{68}-to-Val substitution (Ad-NEU1–G68V). Because Pa expresses its own neuraminidase, NanPs (35, 36), we administered equivalent inocula of WT PAO1 or its NanPs-deficient isogenic mutant, PAO1/$NanPs^-$ (35). Both Pa strains evoked comparable *in vivo* MUC1-ED shedding (Fig. 4*H*). NanPs, a noncanonical neuraminidase, reportedly displays weak catalytic activity (35, 36). In fact, we detected low total sialidase activity for the 4-MU-NANA substrate in extracts of WT PAO1 and comparable modest levels of neuraminidase activity in extracts of PAO1/$NanPs^-$ bacteria.[3]

The full-length MUC1 protein is synthesized as a single polypeptide chain that is proteolytically cleaved at a Gly-Ser peptide bond located 58 aa upstream of the transmembrane domain within the extracellular juxtamembranous region (9, 10). This proteolysis permits shedding of MUC1-ED from the airway EC surface. To establish the role of the Gly-Ser protease recognition site in NEU1-responsive MUC1-ED shedding, HEK293 cells expressing either the WT MUC1-ED or a protease-resistant MUC1-ED S317A mutant were infected with Ad-NEU1 and shed MUC1-ED levels in cell culture supernatants quantified by ELISA. The MUC1-ED S317A mutant contains a Ser-to-Ala substitution within the Gly-Ser site (37). Under conditions of NEU1 overexpression, shedding of WT MUC1-ED was dramatically increased, whereas shedding of the MUC1-ED S317A mutant was nonexistent (Fig. 4*I*). These combined data indicate that 1) catalytically active NEU1 is necessary and sufficient for Pa-provoked MUC1-ED desialylation and shedding *in vivo*; 2) NEU1 overexpression, even in the absence of the Pa stimulus, increases MUC1-ED shedding; 3) Pa-expressed NanPs is not required for or contributory to Pa-induced MUC1-ED desialylation/shedding; and 4) NEU1-driven MUC1-ED shedding requires the Gly-Ser protease recognition site.

Decoy receptor function in MUC1-ED– enriched murine BALF

Because Pa administration to mice dramatically increases shedding of MUC1-ED in their airways (Fig. 1, *A–C*), we asked whether endogenous generation of the soluble MUC1-ED receptor might target one or more flagellin-driven processes that contribute to Pa pathogenicity. At the indicated times postadministration of Pa (1.0×10^5 CFUs/mouse) or PBS, BALF was collected and tested for its ability to influence flagellin binding or Pa adhesion to NEU1-overexpressing human airway ECs or flagellin-driven Pa motility. BALFs harvested from PAK-challenged mice after 2–12 h did not alter flagellin binding, Pa adhesion, or Pa motility compared with the respective controls (Fig. 5, *A–C*). In contrast, BALFs harvested from Pa-challenged mice at 24 h and 48 h reduced flagellin binding (Fig. 5*A*) and Pa adhesion (Fig. 5*B*) to airway ECs by up to 44 and 33%, respectively, and flagellin-driven Pa motility by up to 33% (Fig. 5*C*). By 72 h, the BALF inhibitory activities had disappeared. These time requirements for the inhibitory effects paralleled the appearance of high levels of MUC1-ED in the BALF (Fig. 1*A*). When 48-h BALF samples were incubated with anti-murine MUC1-ED antibody (Ab) or a species- and isotype-matched Ab control (Fig. 5*D*), the inhibitory activities were removed by MUC1-ED immune depletion, but not by incubation with the irrelevant control Ab (Fig. 5, *A–C*). Finally, these same MUC1-ED– containing BALFs displayed no growth inhibitory activity for PAK (Fig. S3*A*). These findings indicate that the shed MUC1-ED endogenously generated within the murine bronchoalveolar compartment acts as decoy receptor to diminish flagellin binding and Pa adhesion to airway epithelia and disrupt Pa motility, *i.e.* flagellin-driven processes that contribute to Pa pathogenesis.

Galectins do not influence the flagellin–MUC1-ED interaction

Galectins are a family of endogenous lectins that contain conserved carbohydrate recognition domains with specificity for β-galactosides (38). β-galactosides are often the penultimate sugar to which the terminally positioned sialic acid residue is tethered (39). Removal of the terminal sialic acid unmasks and increases accessibility of the β-galactosides to galectins. Of the 15 known mammalian galectins, galectin-3 binds to and alters MUC1 function (40, 41). Because MUC1-ED desialylation increases its adhesiveness for flagellin-expressing Pa (Fig. 5*B*), we asked whether one or more galectins might participate in the flagellin–MUC1-ED interaction. Flagellin binding and Pa adhesion to NEU1-overexpressing human airway ECs were assayed in the presence of increasing concentrations of lactose, a broad-spectrum competitive inhibitor of galectins (42). Lactose at concentrations of up to 100 mM failed to diminish flagellin binding or Pa adhesion to the airway ECs (Fig. S4, *A* and *B*). Because MUC1-ED– enriched BALFs inhibit flagellin binding and Pa adhesion to airway ECs (Fig. 5, *A* and *B*), we asked whether galectins might contribute to MUC1-ED decoy receptor function. Although the MUC1-ED– containing murine BALFs dose-dependently inhibited flagellin binding and Pa adhesion to NEU1-overexpressing human airway ECs, the presence of increasing concentrations of lactose did not alter BALF decoy receptor function (Fig. S4, *C* and *D*). These data do not support a role for galectins in the flagellin–MUC1-ED interaction and MUC1-ED decoy receptor function in BALF.

Inhibitory portion of human MUC1-ED decoy receptor: Glycan versus protein backbone

Generation of endogenous murine MUC1-ED in BALF conferred inhibitory activity against flagellin binding and Pa adhesion to airway ECs and Pa motility (Fig. 5, *A–C*). To increase relevance to human disease, we initiated studies with human MUC1-ED. Human MUC1-ED was prepared from supernatants of A549 airway ECs infected with Ad-NEU1, Ad-NEU1-G68V, or Ad-encoding GFP (Ad-GFP) and tested for its ability to inhibit Pa adhesion to fresh monolayers of A549 cells. Incubation with MUC1-ED harvested from Ad-NEU1–infected ECs reduced adhesion by >60% compared with MUC1-ED prepared from Ad-NEU1-G68V– or Ad-GFP–infected cells (Fig. 6*A*). That NEU1-mediated MUC1-ED desialylation increased its inhibitory activity for Pa adhesion indicated that the removed sialic acid residues were not required for MUC1-ED decoy receptor function and that removal of sialic acid unmasks one or more cryptic binding sites for Pa. To determine whether

[3] S. W. Hyun, unpublished results.

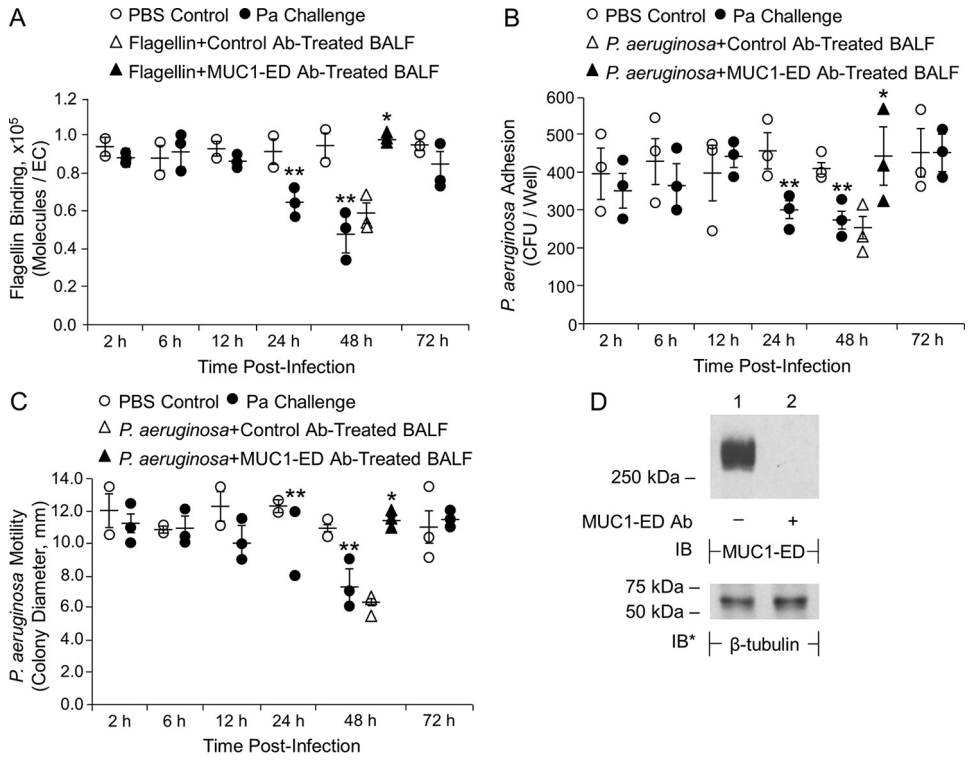

Figure 5. MUC1-ED–enriched BALF inhibits flagellin binding and Pa adhesion to airway ECs and Pa motility. BALB/c mice were administered i.n. with 1.0×10^5 CFUs/mouse of PAK or the PBS vehicle. At increasing times postadministration, BALF was collected. *A* and *B*, A549 cells were infected with Ad-NEU1 (m.o.i. = 100) and cultured for 48 h. *A*, Alexa Fluor 594–labeled flagellin was incubated for 30 min at 4 °C with BALF from uninfected or PAK-infected mice and assayed for binding to Ad-NEU1–infected A549 cells. *B*, PAK was incubated for 30 min at 4 °C with BALF from uninfected or PAK-infected mice and assayed for adhesion to Ad-NEU1–infected A549 cells. *C*, PAK was incubated for 30 min at 4 °C with BALF from uninfected or PAK-infected mice and assayed for bacterial motility. *A–C*, *error bars* represent mean ± S.E. flagellin binding or Pa adhesion or motility ($n = 3$). *D*, BALFs incubated with anti-MUC1-ED or control Abs were processed for MUC1-ED immunoblotting. To control for equal protein and loading, the blot was stripped and reprobed for β-tubulin. Molecular masses in kDa are indicated on the *left*. *IB*, immunoblot; *IB**, immunoblot after stripping. *A–C*, in selected experiments, BALF from PAK-infected mice collected at 48 h postinfection was incubated with anti-MUC1-ED Ab or a species- and isotype-matched nonimmune IgG control. Igs were immobilized on protein G–agarose and removed by centrifugation. The MUC1-ED–immunodepleted or control IgG-treated BALFs were incubated with Alexa Fluor 594–flagellin or Pa, and processed for (*A*) flagellin binding or (*B*) bacterial adhesion to Ad-NEU1–infected A549 cells or (*C*) bacterial motility. *, increased flagellin binding, or Pa adhesion or motility, following incubation with MUC1-ED–immunodepleted BALFs compared with nonimmune IgG-treated BALFs at $p < 0.05$. **, decreased flagellin binding or Pa adhesion or motility following incubation with BALFs from Pa-infected mice compared with incubation with BALF from uninfected controls at $p < 0.05$. The results are representative of three independent experiments.

either of the MUC1-ED glycans immediately subterminal to sialic acid, *i.e.* galactose (Gal) or *N*-acetylgalactosamine (GalNAc), might be required for its binding to flagellin-expressing Pa, PAK was preincubated with these two monosaccharides, either separately or in combination, and assayed for adhesion. Neither glycan blocked Pa adhesion to the ECs (Fig. 6*B*). We next asked whether the MUC1-ED decoy receptor activity might reside within other sugars within its *N*-linked or *O*-linked glycans. Here, MUC1-ED was prepared from supernatants of airway ECs cultured in the presence of the *N*-glycosylation inhibitor, tunicamycin, the *O*-glycosylation inhibitor, benzyl-*N*-acetyl-α-galactosaminide (GalNAc-*O*-bn), or the PBS vehicle. Incubation of PAK with MUC1-ED prepared from tunicamycin-treated cells did not alter adhesion, whereas incubation with MUC1-ED prepared from GalNAc-*O*-bn–treated cells reduced adhesion by ~90%, compared with the PBS vehicle (Fig. 6*C*). Because *E. coli* lack the cellular machinery required for robust posttranslational *N*- or *O*-glycosylation that occurs in eukaryotic systems (43), MUC1-ED was prepared from *E. coli* transformed with a human MUC1 expression plasmid (37). Incubation of PAK with the *E. coli*– expressed human recombinant MUC1-ED reduced adhesion by >95% compared with the empty vector control (Fig. 6*D*). Quantitative MUC1-ED immunoblotting of lysates of airway ECs cultured in the presence of PBS, tunicamycin, or GalNAc-*O*-bn, or *E. coli*–expressed rMUC1-ED, was performed using an Ab raised against the human MUC1-ED protein backbone (44), common to the MUC1-ED preparations used in all four treatment groups. MUC1-ED harvested from ECs cultured in the presence of PBS or tunicamycin displayed comparable relative abundance and gel mobilities (Fig. 6*E*, *lanes 1* and *2*), indicative of the low level of *N*-linked glycosylation in the MUC1-ED. Similarly, MUC1-ED prepared in ECs cultured in the presence of GalNAc-*O*-bn and rMUC1-ED expressed in *E. coli*, two conditions in which *O*-linked glycosylation is greatly reduced, also displayed comparable relative abundance and gel mobilities (Fig. 6*E*, *lanes 3* and *4*). However, the gel mobilities of MUC1-ED prepared under conditions of reduced *O*-linked glycosylation (Fig. 6*E*, *lanes 3* and *4*) were dramatically increased compared with MUC1-ED synthesized in the presence of tunicamycin and the PBS control (Fig. 6*E*, *lanes 1* and *2*) because of the preponderance of *O- versus N*-glycosylation. These findings demonstrate that the decoy receptor function of MUC1-ED does not reside within its *N*- or *O*-linked carbohydrates, but rather, within its protein backbone.

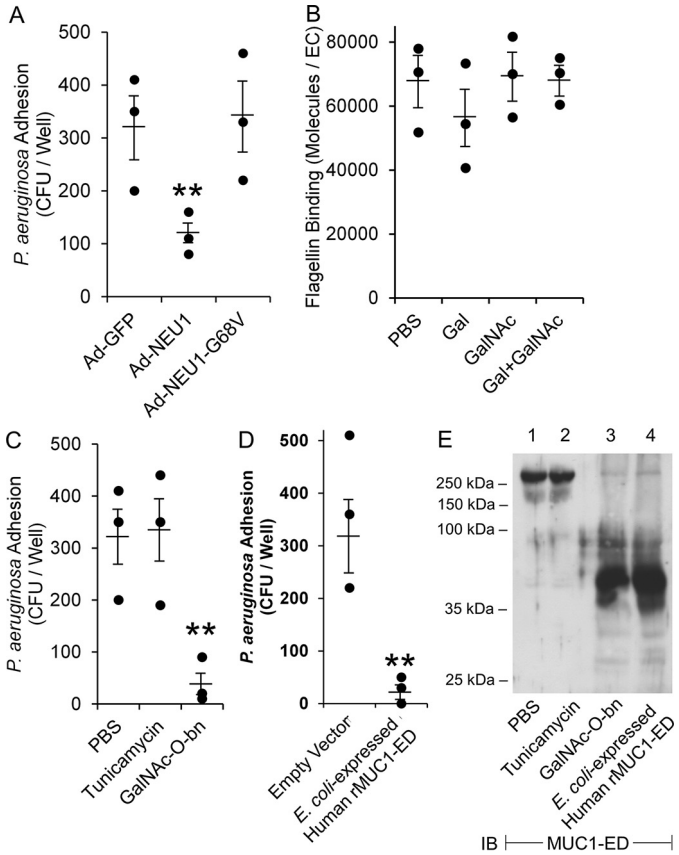

Figure 6. Deglycosylated protein backbone of human MUC1-ED inhibits Pa adhesion to human airway ECs. *A*, PAK was incubated with human MUC1-ED isolated from supernatants of A549 airway ECs infected with Ad-NEU1, Ad-NEU1–G68V, or Ad-GFP (m.o.i. = 100), washed, and assayed for adhesion to fresh, unmanipulated A549 cells ($n = 3$). *B*, Alexa Fluor 594–labeled PAK flagellin was incubated for 30 min at 37 °C with 25 mM of Gal or GalNAc, 25 mM Gal plus 25 mM GalNAc, or the PBS vehicle control. The ECs were washed and processed for flagellin binding by fluorometry ($n = 3$). *C*, PAK was incubated with human MUC1-ED isolated from the supernatants of A549 cells cultured in the presence of 1.0 μg/ml tunicamycin, 5.0 μM GalNAc-*O*-bn, or the PBS vehicle control, washed, and assayed for adhesion to fresh, unmanipulated A549 cells ($n = 3$). *D*, PAK was incubated with human rMUC1-ED prepared from *E. coli* transformed with a MUC1 expression plasmid or the empty vector control, washed, and assayed for adhesion to A549 cells ($n = 3$). *Error bars* represent mean ± S.E. Pa adhesion (*A*, *C*, *D*) or flagellin binding (*B*). **, significantly decreased Pa adhesion *versus* Ad-GFP, PBS, or empty vector controls at $p < 0.05$. *E*, human MUC1-ED isolated from A549 cells cultured in the presence of 1.0 μg/ml tunicamycin, 5.0 μM GalNAc-*O*-bn, or the PBS vehicle control, and *E. coli*-expressed human rMUC1-ED were processed for MUC1-ED immunoblotting. Molecular masses in kDa are indicated on the *left*. *IB*, immunoblot. The results are representative of three independent experiments.

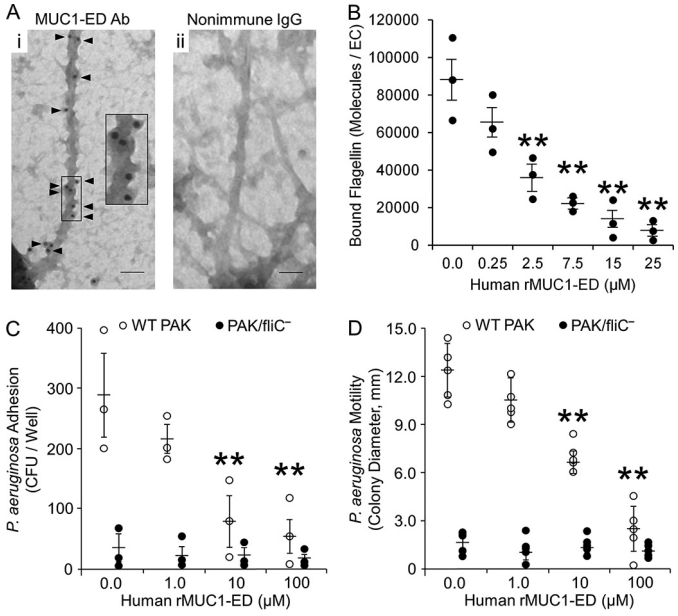

Figure 7. Human rMUC1-ED inhibits flagellin binding and Pa adhesion to human airway ECs and Pa motility. *A*, PAK was incubated with 25 μM of human rMUC1-ED for 1 h at 4 °C. The bacteria were incubated with mouse anti-MUC1-ED Ab (*panel i*) or nonimmune mouse IgG (*panel ii*), each at 1:5000 dilution, for 1 h at 4 °C, followed by gold-labeled goat anti-mouse IgG secondary Ab at 1:10,000 dilution for 1 h at 4 °C, and examined by transmission immunoelectron microscopy. Each section was photographed at 11,000× or 44,000× (*insert*). *Arrowheads* indicate immunogold labeling. *Scale bar*, 100 nm. *B* and *C*, Human rMUC1-ED at the indicated concentrations or the PBS vehicle control were incubated with (*B*) Alexa Fluor 594–labeled Pa flagellin ($n = 3$) or (*C*) WT PAK or the flagellin-deficient PAK/fliC$^-$ mutant ($n = 3$) and assayed for (*B*) flagellin binding or (*C*) Pa adhesion to Ad-NEU1–infected A549 cells. *D*, the indicated concentrations of human rMUC1-ED or the PBS vehicle control were incubated with WT PAK or the PAK/fliC$^-$ mutant, and the bacteria were stab-inoculated into 0.3% agar plates and incubated overnight. Pa colony diameter was measured as an indicator of bacterial motility ($n = 3$). *Error bars* represent mean ± S.E. flagellin binding (*B*), Pa adhesion (*C*), or Pa motility (*D*). **, significantly decreased flagellin binding or Pa adhesion or motility *versus* the PBS control at $p < 0.05$. The results are representative of three independent experiments.

Bioactivities of E. coli–derived human rMUC1-ED in vitro

Endogenous murine MUC1-ED in BALF diminishes flagellin binding and Pa adhesion to airway ECs, and Pa motility (Fig. 5, *A–C*), and *E. coli*–derived human rMUC1-ED profoundly reduces Pa adhesion (Fig. 6*D*). To further validate the utility of *E. coli*–derived human rMUC1-ED as a Pa flagellin-targeting intervention, we used immunogold EM to establish its binding to the intact Pa flagellum (Fig. 7*A*). We observed anti–MUC1-ED Ab immunolocalized to the PAK flagellar filament following incubation of the bacteria with human rMUC1-ED (Fig. 7*A*, *panel i*), but not to bacteria incubated with rMUC1-ED and a nonimmune mouse IgG (Fig. 7*A*, *panel ii*). We then tested the inhibitory activity of human rMUC1-ED for flagellin binding, Pa adhesion, and Pa motility. Human rMUC1-ED dose-dependently inhibited flagellin binding by >90% (Fig. 7*B*) and flagellin-expressing WT PAK adhesion to human airway epithelia by up to 85% (Fig. 7*C*), and WT PAK motility by >80% (Fig. 7*D*). As negative controls, human rMUC1-ED had no effect on adhesion (Fig. 7*C*) or motility (Fig. 7*D*) of PAK/fliC$^-$. However, human rMUC1-ED displayed no effect on the growth of flagellin-expressing PAK (Fig. S3*B*). Thus, human rMUC1-ED exhibited robust, flagellin-targeting decoy receptor function without inhibiting Pa replication.

Efficacy of E. coli–derived human rMUC1-ED in a mouse model of Pa pneumonia

E. coli–expressed human rMUC1-ED competitively inhibits flagellin binding and Pa adhesion to human airway ECs, and Pa motility (Fig. 7, *B–D*), *in vitro*. To address whether human rMUC1-ED might provide *in vivo* protection in a murine model of acute Pa pneumonia, mice were administered a sublethal dose of WT PAK (1.0×10^5 CFUs/mouse) or PBS, in the presence of increasing concentrations of human rMUC1-ED. BALF and lungs were harvested for Pa CFUs/mg lung tissue and Pa CFUs/mg BALF protein, BALF TNFα and KC levels, and lung MPO activity. Human rMUC1-ED dose-dependently decreased

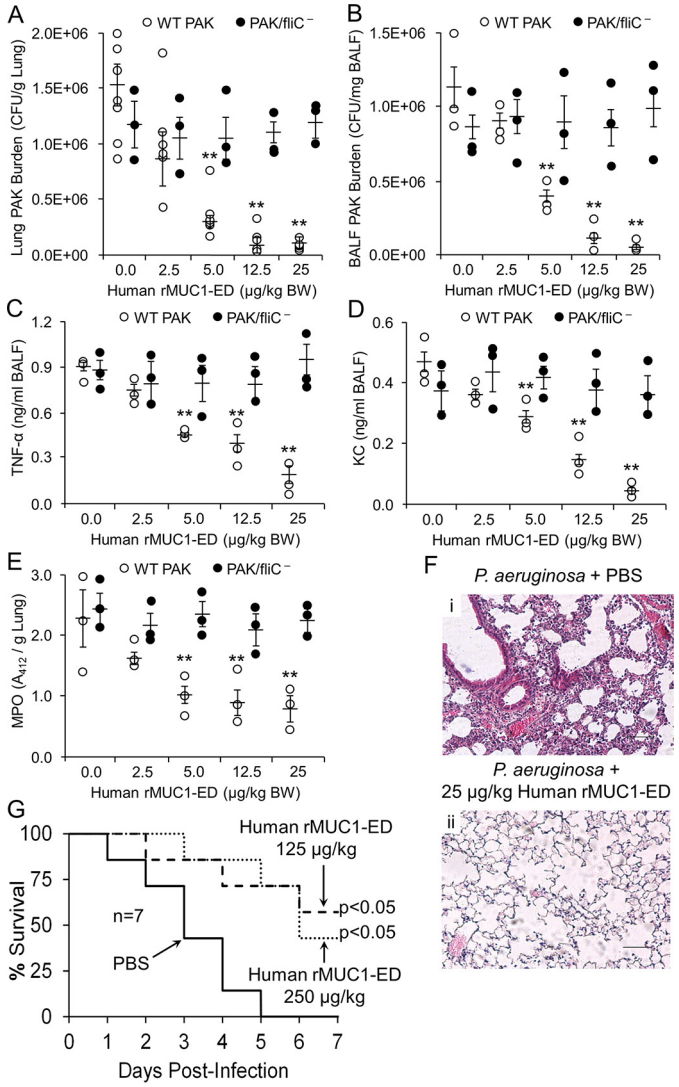

Figure 8. Human rMUC1-ED protects against lethal Pa lung infection. WT PAK or the PAK/fliC$^-$ mutant (1.0×10^5 CFUs/mouse) were co-administered i.n. with PBS or 2.5, 5.0, 12.5, or 25 μg/kg body weight (BW) of human rMUC1-ED to BALB/c mice. *A–E*, lung (*A*) and BALF CFUs (*B*), TNFα (*C*) and KC (*D*) levels in BALF, and lung MPO (*E*) levels were measured at 24 h postinfection. *Error bars* represent the mean ± S.E. Pa CFUs/g lung protein or CFUs/mg BALF protein, TNFα ng/ml and KC ng/ml BALF, or MPO activity/g lung protein ($n = 3$). **, reduced WT PAK CFUs, TNFα, KC, or MPO following Pa co-administered with human rMUC1-ED *versus* the PBS controls at $p < 0.05$. *F*, WT PAK (1.0×10^5 CFUs/mouse) was co-administered i.n. with PBS (*panel i*) or 25 μg/kg BW of human rMUC1-ED (*panel ii*) to BALB/c mice. At 24 h postinfection, lungs were harvested and sections were stained with hematoxylin and eosin, and examined by microscopy. Each section was photographed at 400×. *Scale bar*, 50 μM. The photomicrographs are representative of three mouse lung sections. *G*, WT PAK (2.0×10^7 CFUs/mouse) was co-administered i.n. with PBS, or 125 or 250 μg/kg BW of human rMUC1-ED to BALB/c mice and survival was measured daily by Kaplan-Meier analysis ($n = 7$/group). The results are representative of three independent experiments.

the WT PAK lung burden by >90% (Fig. 8*A*) and BALF WT PAK CFUs by >95% (Fig. 8*B*), TNFα (Fig. 8*C*) and KC (Fig. 8*D*) concentrations in the BALF by >75% and >90%, respectively, and pulmonary leukostasis as measured by lung MPO activity by up to 65% (Fig. 8*E*), compared with these same end points in mice administered PAK alone. In contrast, human rMUC1-ED had no effect on lung (Fig. 8*A*) or BALF (Fig. 8*B*) CFUs, TNFα (Fig. 8*C*) or KC (Fig. 8*D*) levels in the BALF, or lung MPO activity (Fig. 8*E*) when co-administered with 1.0×10^5 CFUs/mouse of the PAK/fliC$^-$ mutant. In fact, PAK/fliC$^-$ displayed identical growth curves to the flagellin-expressing WT PAK (Fig. S3*C*). Co-administration of WT PAK with human rMUC1-ED to mice also dramatically reduced inflammatory cells in hematoxylin and eosin–stained lung sections compared with mice administered PAK alone (Fig. 8*F*). In survival studies, co-administration of WT PAK with human rMUC1-ED at 125 μg/kg or 250 μg/kg improved survival compared with mice co-administered PAK plus the PBS control (Fig. 8*G*). At 5 days postinfection, mice administered PAK with human rMUC1-ED exhibited >70% survival *versus* 0% survival in mice administered PAK with PBS. These data support the potential therapeutic value for *E. coli*–derived human rMUC1-ED for invasive lung infection by flagellin-expressing Pa.

Discussion

The MUC1-ED sialylation state is dynamically and coordinately regulated through the opposing catalytic activities of sialyltransferases and sialidases (19, 20, 45). We previously demonstrated intense NEU1 immunostaining at the superficial surface of the human airway epithelium, including the brush border of the trachea and bronchus (19). This NEU1 expression pattern closely correlated with that previously established for the MUC1-ED in these same tissues (46). In cultured human airway epithelia, forced NEU1 overexpression profoundly desialylated the MUC1-ED (19, 20). Of course, supraphysiological levels of NEU1 may indiscriminately desialylate sialoproteins, including the MUC1-ED. However, NEU1 depletion dramatically increased MUC1-ED sialylation, indicating that in resting cells, ongoing constitutive NEU1-mediated MUC1-ED desialylation occurs (19, 20). In these same studies, silencing of NEU1 completely protected against flagellin-induced MUC1-ED shedding. We speculated that NEU1-mediated MUC1-ED desialylation unmasks the Gly-Ser protease recognition site, increasing its susceptibility to proteolysis by MUC1-ED sheddases (20). In fact, although forced NEU1 overexpression increased shedding of WT MUC1-ED, it did not increase shedding of the protease-resistant MUC1-ED S317A mutant. Further, we have established expression of two of the three known MUC1-ED sheddases (21–23), matrix metalloproteinase-14 and γ-secretase, in human airway epithelia (20). These combined data indicate that MUC1-ED shedding is regulated, at least in part, through NEU1-mediated MUC1-ED desialylation and unmasking of the Gly-Ser protease recognition site.

We asked which Pa constituents or byproducts were required to provoke MUC1-ED shedding. In mice challenged with PAK, inocula of $\geq 5.0 \times 10^3$ CFUs/mouse increased MUC1-ED shedding. In these same mice, the Pa lung burden peaked at 24 and 48 h. Hence, the time points when MUC1-ED shedding peaked were temporally coincident with lung Pa colony counts that exceeded the threshold established for Pa-stimulated MUC1-ED shedding. Both types of flagellin expressed by Pa, FlaA and FlaB, provoked comparable MUC1-ED shedding. Although the overall aa sequence identity between the 394 aa FlaA and 488 aa FlaB proteins is only 47% (47, 48), several sequences, including the NH_2-terminal aa 1–229 and C-terminal aa 366–488, display ≥60% identity, and both flagellins have identical sequences between aa 1–19, 37–50, 67–91, and 462–482. Because the two flagellin types induce similar MUC1-ED

shedding, it is conceivable that one or more of these shared sequences engage the MUC1-ED to induce shedding. When mice were challenged with equivalent inocula of the PAK strain or its PAK/fliC^{-} isogenic mutant, MUC1-ED shedding was dramatically reduced in animals challenged with the Pa strain lacking flagellin. Similarly, incubation of Pa with anti-flagellin antisera profoundly reduced Pa-induced MUC1-ED shedding. These results underscore the central role for Pa flagellin in MUC1-ED shedding. However, the flagellin-deficient mutant still modestly increased shedding compared with the simultaneous PBS control, indicating that Pa constituents other than flagellin might also be contributory.

That elevation of TNFα and KC levels in BALF temporally coincided with increases in lung MPO activity raises the possibility that TNFα-induced increases in endothelial expression of one or more leukocyte-endothelial adhesion molecule(s) (49) and/or the generation of KC chemotactic gradients (50) might, in part, explain the increase in pulmonary leukostasis. That the increase in lung MPO activity coincided with increases in MUC1-ED shedding raises the possibility that one or more proteases provided by recruited neutrophils (51, 52) might participate in the proteolytic processing and release of MUC1-ED.

We failed to detect up-regulation of NEU1/PPCA expression or activity in response to a Pa/flagellin stimulus *in vivo*. Although potential positive and negative *cis*-acting elements have been identified in the murine *NEU1* gene promoter (53), the mechanism(s) through which NEU1 expression is regulated remains unknown. That flagellin stimulation of cultured airway ECs provokes MUC1-ED desialylation within 30 min (20) argues against *de novo* NEU1 protein synthesis as an explanation for altered NEU1 catalytic activity. Translocation of preformed pools of NEU1 and/or its chaperone/transport protein, PPCA, to the surface-expressed MUC1-ED substrate remains a possibility. First described as a lysosomal enzyme (18), NEU1 has been detected on the surface of multiple cell types (54–58). Surface-expressed NEU1 can associate with and/or desialylate multiple surface glycoproteins, including CD31 (59), TLR4 (60), and receptors for EGF (19), elastin (61), platelet-derived growth factor BB (62), insulin (63), and insulin growth factor (62, 63).

Although catalytically active NEU1 has been detected on the cell surface (58, 64), the mechanisms through which it may be translocated to a membrane-tethered substrate are incompletely understood. NEU1 might exit the cell via lysosomal exocytosis. However, NEU1 is a negative regulator of lysosomal exocytosis (65). A tyrosine-containing internalization motif in the C terminus of NEU1, aa 412–415, reportedly targets the enzyme to the lysosome (54). Upon NEU1 Tyr^{412} phosphorylation in activated lymphocytes, NEU1 is redistributed to the cell surface. In human lung microvascular endothelia, cell-cell contact increases NEU1 association with and desialylation of CD31 (59). As these cells achieve confluence and their surface-expressed CD31 EDs homophilically engage, Src family kinases are activated to increase tyrosine phosphorylation of p120catenin, which in turn, becomes a cross-bridging adaptor molecule that physically couples NEU1 to CD31. NEU1 has been detected within exosomes released from murine microglial cells (66). More recently, two putative transmembrane domains have been described in human NEU1, which would be compatible with its retention within the plasma membrane (67). In human airway ECs, Pa/flagellin treatment increases MUC1 co-immunoprecipitation of NEU1 and its chaperone PPCA (20). We now have extended these findings to an *in vivo* mouse model where Pa administration increases NEU1-MUC1 and PPCA-MUC1 association in lung tissue, as seen in reciprocal co-immunoprecipitation assays. The specific pathway through which NEU1 might gain access to the cell surface and the MUC1-ED substrate is unknown.

NEU1-mediated MUC1-ED desialylation was evident for MUC1-ED harvested from BALF, but not from lung homogenates. These findings indicate that desialylated MUC1-ED is more susceptible to proteolytic processing and release into the BALF, whereas sialylated MUC1-ED is more resistant and remains cell-associated. NEU1-selective and broad-spectrum sialidase inhibition each almost completely eliminated MUC1-ED desialylation *in vivo*, but diminished MUC1-ED shedding by no more than 55%, compared with the simultaneous uninhibited controls. We previously reported this same differential response in cultured human airway ECs *in vitro*, in terms of MUC1-ED desialylation *versus* shedding (20). Although the MUC1-ED contains numerous, terminally sialylated *O*-glycan chains extending from its tandem repeats, given the rodlike structure of the MUC1-ED that can extend up to 500 nm above the cell surface (11), only a small fraction of its sialylated glycans are likely to mask the Gly-Ser protease recognition site located in its juxtamembranous region. It is only in this region that the glycan chains are *N*-linked (9, 11). Our PNA pulldown strategy does not discriminate between those sialylated glycan chains that mask the proteolytic site and those that do not. Therefore, the sialidase inhibitors may protect against removal of a large number of sialic acid residues that are spatially removed from the Gly-Ser protease recognition site, and do not participate in masking this site from MUC1-ED sheddases. A much smaller proportion of those specific glycan chains expressed in close proximity to the site of proteolysis would be impacted. Whether differences in the location of a specific sialic acid linkage, and therefore the site of NEU1 activity and sialic acid removal, influences the ability of either of the two sialidase inhibitors to access the NEU1 catalytic pocket is unknown.

Bacterial adhesion to host epithelia is a prerequisite to establishment of invasive infection and is mediated through interactions between microbial adhesins and their cognate host cell receptors (3). Pa flagellin contributes to Pa virulence through increased motility, adhesion, and invasion (2). Any host factor capable of disrupting these flagellin-driven processes would be predicted to protect against Pa pathogenesis. In the current studies, the flagellin-targeting, desialylated MUC1-ED decoy receptor diminished binding of Pa-derived flagellin and adhesion of viable Pa to airway epithelia and Pa motility *in vitro*. Further, co-administration of human rMUC1-ED with Pa to mice dramatically reduced Pa lung burden, Pa-provoked increases in proinflammatory cytokine expression, pulmonary leukostasis, and mouse mortality. The MUC1-ED is highly glycosylated through >500 predicted *O*-linked glycosylation sites within its tandem repeats, but only five predicted *N*-linked glycosylation sites within the juxtamembranous region (9, 10, 12).

Therefore, *O*-glycans are responsible for >99% of MUC1-ED glycan chains. On the basis of relative abundance, and perhaps to a lesser degree, differential localization, it is not surprising that modulation of *O*-linked glycosylation with GalNAc-*O*-bn has far greater impact on decoy receptor function than does alteration of *N*-linked glycosylation through tunicamycin treatment. Finally, expression of human rMUC1-ED in a prokaryotic system, in which neither *O*- nor *N*-linked glycosylation is robust (43), generates a highly inhibitory decoy receptor. Our interpretation of these combined data is that MUC1-ED glycosylation is not required for its recognition of Pa flagellin and decoy receptor function. In fact, it is these sialylated glycan structures that mask the MUC1-ED protein backbone in which the binding sites for Pa-derived flagellin resides.

The mechanism(s) through which the MUC1-ED decoy receptor influences the outcome of the Pa–host interaction remain incompletely understood. Through its ability to interrupt flagellin-driven Pa motility, the MUC1-ED may interfere with Pa penetration of the mucus blanket (68), invasion of the first-line epithelium (19), movement through the paracellular pathway into subepithelial tissues (69), and, finally, Pa resistance to mucociliary clearance (70). Inhibition of flagellin-dependent Pa adhesion to the host epithelium likely decreases Pa colonization of the airway and may impair its engagement of host EC receptors and invasion of the epithelium. Disruption of the MUC1-ED–Pa flagellin receptor-ligand interaction likely blocks MUC1-driven downstream intracellular signaling (8), biosynthesis of proinflammatory cytokines/chemokines (71, 72), and neutrophil recruitment to the bronchoalveolar compartment (72). Flagellin-provoked, NEU1-mediated MUC1-ED desialylation, and conceivably desialylation of other airway mucins, may well alter mucus viscosity, which in turn might influence mucociliary clearance. Disruption of Pa–host cell adhesion and removal of sialic acid residues from the MUC1-ED with their release into the airway lumen may influence formation of sialic acid–rich glycocalyces, known to contribute to Pa pathogenesis (35, 73).

The current data establish a novel host defense mechanism specific for Pa-derived flagellin with generation of a MUC1-ED decoy receptor at the airway epithelial surface. Whether this schema can be extended to 1) other flagellated respiratory pathogens (*e.g. Legionella pneumophila*, *Stenotrophomonas maltophilia*), 2) extrapulmonary mucosal surfaces (*e.g.* the gastrointestinal and genitourinary tracts), 3) membrane-tethered airway mucins other than MUC1 (*e.g.* MUC4, MUC16), 4) other sialylated receptors and surface-expressed sialoproteins (*e.g.* EGFR, CD31, TLR4, elastin receptor complex, and receptors for platelet-derived growth factor-BB, insulin, and insulin growth factor), 5) other host sialidases (*e.g.* NEU3) and prokaryotic neuraminidases (*e.g.* influenza virus, *Streptococcus pneumoniae*), and/or 6) sialic acid–rich biofilm formation are unknown. Within the context of cystic fibrosis, our data suggest that down-regulation of flagellin-expression by Pa in the cystic fibrosis lung (74–77) might contribute to reduced MUC1-ED shedding and possibly decreased host defenses against Pa colonization and/or infection. Finally, our data establish the MUC1-ED decoy receptor as a mechanistically novel host response that may be harnessed as a therapeutic intervention to target Pa, including multidrug-resistant strains.

Experimental procedures

Reagents

All reagents were from Sigma-Aldrich unless otherwise noted. Rabbit anti-mouse MUC1-ED Ab (catalogue no. LS-C343984) was from LifeSpan BioSciences. Mouse anti-human MUC1-ED (catalogue no. MA1–06503), hamster anti-human MUC1-CD (catalogue no. MA5–11202), and rabbit anti-mouse NEU1 (catalogue no. PA5–42552) Abs; nonimmune mouse IgG (catalogue no. 02–6502); and nickel-nitrilotriacetic acid agarose were from Thermo Fisher. Rabbit anti-mouse PPCA (catalogue no. ab217857), rabbit anti-human NEU1 (catalogue no. ab111752), and rabbit anti-human PPCA (catalogue no. ab181129) Abs were from Abcam. Rabbit anti-mouse β-tubulin (catalogue no. PA5–16863), mouse anti-human β-tubulin (catalogue no. MA5–16308) Abs, horseradish peroxidase (HRP)–conjugated rabbit anti-mouse IgG (catalogue no. 61–6520), HRP-conjugated goat–anti-rabbit IgG (catalogue no. 65–6120), and HRP-conjugated goat anti-hamster IgG (catalogue no. PA1–29626) Abs were from Thermo Fisher. PNA and PNA-agarose were from Vector Laboratories. DANA was from Calbiochem. C9-BA-DANA was prepared as described (78).

Bacteria

The laboratory and clinical Pa strains used in this study are listed in Table S1. Clinical strains of Pa were isolated as part of routine clinical care from patients with pneumonia as determined by the presence of pulmonary infiltrates on chest X-ray, and/or computerized axial tomography, and the presence of Gram-negative bacilli in sputum samples that cultured positive for Pa. All Pa strains were grown at 37 °C at 200 rpm in Luria-Bertani (LB) broth (10 mg/ml tryptone, 5.0 mg/ml yeast extract, 10 mg/ml NaCl) and quantified spectrophotometrically at A_{600}.

Purification of Pa and Salmonella Typhimurium flagellins

Pa-derived flagellin was purified and adsorbed with polymyxin B–agarose to remove bacterial LPS, after which less than 0.1 LPS units/μg of protein was detected by the Limulus amebocyte lysate assay as described (20). Flagellin was purified from STm strain CVD1925, a derivative of the WT invasive Malian strain I77, as described (79, 80). Both Pa and STm flagellins exhibited a single Coomassie Blue–stained protein band following SDS-PAGE.

Purification of and preparation of antisera to Pa rFlaA and rFlaB flagellins

The DNA sequences of *FlaA* (GenBank accession no. CP020659.1) and *FlaB* (GenBank accession no. AE004091.2) from PAK and PAO1, respectively, were codon optimized (GenScript) for expression in *E. coli*, cloned into pUC57 and pJET1.2, respectively, and the plasmids transformed into *E. coli* NEB 5-alpha Competent cells (New England Biolabs). The *FlaA* and *FlaB* genes were amplified by PCR, cloned into pTrcHis-TOPO (Thermo Fisher), and expressed in *E. coli* BL21 Compe-

tent cells (New England Biolabs) for production of His_6-tagged rFlaA and rFlaB proteins. Both rFlaA and rFlaB proteins were purified as described (79) and exhibited a single Coomassie Blue–stained protein band following SDS-PAGE. For preparation of mouse polyclonal antisera to rFlaA and rFlaB, 6- to 7-week-old female Crl:CD-1 mice (Charles River Laboratories) were injected in the right gastrocnemius muscle on 0, 14, and 28 days with 2.5 μg of rFlaA or rFlaB flagellins, as described (80). Blood was collected by retro-orbital bleeding at 14 days following the final immunization and centrifuged, and the serum stored at −20 °C.

Murine model of Pa pneumonia

Animal studies were reviewed and approved by the University of Maryland School of Medicine Institutional Animal Use and Care Committee (IACUC) (protocol no. 0617005) and conducted in accordance with guidelines of the Care and Use of Laboratory Animals of the National Institutes of Health. Male and female BALB/c mice (18–20 g) were administered i.n. sublethal (1.0×10^2 to 1.0×10^7 CFUs/mouse) or lethal (2.0×10^7 CFUs/mouse) inocula of WT PAK, PAK/fliC$^-$, WT PAO1, PAO1/NanPs$^-$, Pa clinical strains isolated from patients with pneumonia, or the PBS vehicle, as described (72). In selected experiments, mice were administered purified, LPS-free, Pa flagellin (10 ng/mouse), Pa LPS (100 ng/mouse), Pam_3Cys-Ser-(Lys)4 (10 μg/mouse), or CpG ODN 1826 (10 μg/mouse). In other experiments, mice were treated intraperitoneally with 50–170 nmol/g body weight of the broad-spectrum sialidase inhibitor DANA or the NEU1-selective sialidase inhibitor C9-BA-DANA, as described (30). At each postchallenge time point, mice were euthanized by CO_2 inhalation and cervical dislocation, and BALF and lung tissues harvested as described (72). At 24 h postchallenge, paraffin-embedded lung sections were stained with hematoxylin and eosin, as described (34). Lung tissues were homogenized at 4 °C with a Dounce homogenizer in PBS, pH 7.2, containing 0.1% Triton X-100 and 1% protease inhibitor mixture. The homogenate was centrifuged for 10 min at 10,000 × *g* and the protein concentration of the supernatant measured using the Bradford assay. For BALF collection, pyrogen-free 0.9% NaCl was introduced i.t. in five 1.0-ml aliquots, after which the BALF was retrieved with gentle suction, its volume recorded, and samples placed on ice. After removal of a single aliquot for quantitative Pa cultures in CFUs/ml, the BALF was filtered through sterile gauze, centrifuged at 450 × *g* to remove cells, and the supernatants concentrated 25-fold by passage through membrane filters (pore size 10 kDa) mounted in Centricon tubes (Millipore) as described (20). BALF samples were assayed for TNFα, KC, and shed MUC1-ED levels by ELISA (30, 71), MUC1-ED desialylation with PNA blotting (19, 20), sialidase activity for the fluorogenic 4-MU-NANA substrate (30), and inhibitory activities for Alexa Fluor 594–labeled Pa flagellin binding and Pa adhesion to airway ECs (19, 20), and Pa motility (71). Total lung cellular RNA was extracted and processed for qRT-PCR for normalized NEU1 and PPCA mRNA levels as described (30). Lung homogenates were serially diluted for quantitative bacterial cultures in CFUs/g protein as described (20) and processed for MPO activity as a biochemical marker of neutrophil recruitment (31), reciprocal NEU1-MUC1 and PPCA-MUC1 co-immunoprecipitation assays, and PNA blotting of MUC1-ED immunoprecipitates (20). In selected experiments, equivalent doses of Ad-NEU1or Ad-Null were instilled i.t. in mice as described (34). After 3 days, when maximum NEU1 mRNA expression in mouse lung tissues had been documented (34), mice were euthanized and BALF harvested and assayed for shed MUC1-ED by ELISA and MUC1-ED desialylation with PNA blotting.

ELISAs for murine and human MUC1-ED

Murine BALF or human EC supernatants were centrifuged at 10,000 × *g* for 10 min at 4 °C, added in triplicate to 96-well ELISA plates (MaxiSorb; Nalge Nunc), and incubated overnight at 4 °C. Wells were blocked for 1 h at room temperature with PBS, pH 7.0, containing 10 mg/ml BSA and 50 mg/ml sucrose, and washed with PBS containing 0.05% Tween 20 (PBS-T). The samples were reacted for 2 h at room temperature with 200 μg/ml of rabbit anti-murine or mouse anti-human MUC1-ED antibody, washed with PBS-T, reacted for 2 h at room temperature with 200 μg/ml of HRP-conjugated goat anti-rabbit IgG or HRP-conjugated goat anti-mouse IgG secondary antibody, and washed with PBS-T. Bound antibodies were detected with tetramethylbenzidine substrate (SureBlue, KPL, Inc.). The substrate reaction was stopped with 1.0 N HCl, and A_{450} measured. A standard curve using purified murine or human MUC1-ED was generated for each ELISA plate.

NEU1-MUC1 and PPCA-MUC1 co-immunoprecipitation

Lung homogenates were precleared overnight at 4 °C with protein G–agarose beads and incubated overnight at 4 °C with anti-mouse NEU1, anti-mouse PPCA, or anti-mouse MUC1-CD antibodies. The resultant immune complexes were immobilized by incubation with protein G–agarose for 2 h at 4 °C, centrifuged, washed, boiled in SDS-PAGE sample buffer, and again centrifuged. The supernatants from NEU1 and PPCA immunoprecipitates were processed for MUC1-CD immunoblotting and the supernatants from MUC1-CD immunoprecipitates processed for NEU1 and PPCA immunoblotting. To control for loading and transfer of immunoprecipitates, blots were stripped and reprobed with the immunoprecipitating antibodies. Each NEU1/PPCA signal was normalized to MUC1-CD signal and each MUC1 signal was normalized to NEU1/PPCA signal in the same lane in the same stripped and reprobed blot.

MUC1-ED immunoblotting assays

Equal protein aliquots of BALFs were resolved by SDS-PAGE and transferred to polyvinylidene fluoride (PVDF) membranes. The membranes were probed with rabbit anti-mouse MUC1-ED Ab followed by HRP-conjugated goat anti-rabbit IgG secondary Ab and enhanced chemiluminescence reagents as described (19, 20).

PNA lectin blotting of desialylated MUC1-ED

Equal protein aliquots of BALF and lung homogenates solubilized with lysis buffer as described (19, 20) were incubated with PNA immobilized on agarose beads to selectively enrich for PNA-binding proteins. The PNA-bound proteins were

resolved by SDS-PAGE, transferred to PVDF membrane, and the blots incubated with rabbit anti-murine MUC1-ED antibody, as described (19, 20). Asialofetuin (1.0 μg) was used as a positive control for PNA-binding proteins whereas fetuin (1.0 μg) was used as a negative control.

Cytokine ELISAs

TNFα and KC in murine BALFs were quantified by ELISA using commercially available capture and detection antibodies (R&D Systems), as previously described (72). Briefly, 96-well ELISA plates (Thermo Fisher) containing rabbit anti-mouse TNFα or anti-mouse KC capture antibodies were blocked with PBS, pH 7.2, containing 1% BSA. The plates were washed, and 100 μl of BALF added to each well and incubated for 2 h at 25 °C. The plates were again washed, 100 μl of biotinylated goat anti-rabbit IgG detection antibody added to each well, and the plates incubated for 2 h at 25 °C. The plates were washed, 100 μl of peroxidase-labeled streptavidin added, the plates incubated for 1 h at 25 °C, and developed with 100 μl of tetramethylbenzidine substrate (KPL, Inc.). A_{450} values were measured, and TNFα and KC levels determined from standard curves constructed with serial dilutions of purified standards.

Lung MPO assay

MPO activity in murine lung homogenates was measured using the colorimetric Myeloperoxidase Activity Assay Kit (Abcam) (31). Briefly, 50 μl of lung homogenates were incubated with 40 μl of MPO assay buffer and 10 μl of MPO substrate for 1 h at 25 °C and the reaction stopped with 2.0 μl of MPO assay stop solution. Following incubation for 10 min at 25 °C, 50 μl of 2-thio-5-nitrobenzoate detection reagent was added, the mixture incubated for 10 min at 25 °C, and A_{412} measured.

Flagellin binding to airway ECs

Airway ECs infected with Ad constructs (2.0×10^5 ECs/well) were exposed to Alexa Fluor 594 –labeled flagellin, as described (20). The ECs were washed and bound flagellin was determined by fluorometry (λex = 591 nm, λem = 615 nm). BALF samples containing inhibitory activity for flagellin binding were re-analyzed after either immunodepletion with anti–MUC1-ED antibody or preincubation with a species- and isotype-matched nonimmune IgG control as described (20).

Pa adhesion to airway ECs

Airway ECs infected with Ad constructs (2.0×10^5 ECs/well) in 24-well plates were fixed for 10 min with 2.5% glutaraldehyde in PBS at room temperature and washed three times with PBS, as described (19, 20). Fixed cells were incubated in the presence of BALF, with 2.0×10^7 CFUs/well of Pa in 0.5 ml for 40 min at 37 °C and washed three times with PBS. Bound bacteria were released with 0.05% trypsin, and bound CFUs quantified on LB agar plates. BALF samples containing inhibitory activity for Pa adhesion were re-analyzed after either immunodepletion with anti–MUC1-ED antibody or preincubation with a species- and isotype-matched nonimmune IgG control as described (20).

Pa motility assay

Pa were preincubated with BALF, washed, and resuspended in LB broth. The bacteria were stab-inoculated into 0.3% LB agar plates, incubated overnight, and colony diameters measured as an indicator of bacterial motility, as described (71). BALF samples containing inhibitory activity for Pa motility were re-analyzed after either immunodepletion with anti–MUC1-ED antibody or preincubation with a species- and isotype-matched nonimmune IgG control as described (20).

Adenoviral constructs

Recombinant Ad encoding FLAG-tagged human NEU1 (Ad-NEU1), Ad encoding the catalytically dead NEU1 mutant, Ad-NEU1-G68V, Ad-GFP, and Ad-Null were generated using the AdEasy Adenoviral Vector System (Stratagene, La Jolla, CA) as described (19, 20, 57, 59).

E. coli expression and purification of human rMUC1-ED

Human MUC1-ED incorporating flanking NcoI and EcoRI restriction sites was amplified by PCR from a full-length MUC1-pcDNA3 plasmid (43) and the amplicons subcloned into the multiple cloning site of the pBAD/His plasmid (Invitrogen). The plasmid was transformed into *E. coli* NEB 5-alpha Competent cells (New England Biolabs), the cells were cultured to mid-log phase (A_{600} = 0.5), induced for 3 h with 0.01% arabinose, and lysed by sonication. Human rMUC1-ED was purified on a nickel-nitrilotriacetic acid affinity column, and its identity and purity were verified by immunoblotting with anti-human MUC1-ED Ab and by Coomassie Blue staining.

Immunogold EM

Pa were incubated with 25 μM of human rMUC1-ED for 1 h at 4 °C, fixed with 2% paraformaldehyde for 30 min, and washed three times with 0.1 M phosphate buffer, pH 7.0. The bacteria were adsorbed onto Pioloform-coated 300 mesh nickel grids, inserted into a mPrep/g capsule (Microscopy Innovations), and attached to the mPrep/f couplers fitted in the Z drive of the autosampler of an automated specimen processor ASP-1000 (Microscopy Innovations). Immunoelectron microscopy labeling was performed entirely in the mPrep/g capsule driven by a customized ASP1000 program controlling the sequence of liquid exchanges and timing of incubation. Abs and labeling solutions were predispensed in 96-well plates, and all incubations and washings were agitated by aspirating and dispensing at fixed intervals of 15 to 120 s. The program steps were as follows: 1) quenching in 50 mM glycine in PBS, pH 7.4, for15 min; 2) washing with PBS, pH 7.4, for 5 min; 3) blocking in 2.5% BSA, 0.5% fish gelatin, 0.05% NaN_3, and PBS, pH 7.4, for 30 min; 4) washing two times with 0.2% acetylated BSA, 0.1% fish gelatin, and 0.05% NaN_3 (wash buffer) for 15 min; 5) incubation with anti-MUC1-ED Ab or nonimmune mouse IgG, each diluted 1:5000 in wash buffer, for 2 h; 6) washing four times with wash buffer for 30 min; 7) incubation with 10 nm gold-labeled goat-anti mouse IgG secondary Ab diluted 1:10,000 in wash buffer for 2 h; 8) washing four times with wash buffer and two times with PBS, pH 7.4, for 30 min; 9) fixation with 2% glutaraldehyde in PBS, pH 7.4, for 10 min; 10) washing two times with 0.1 M

phosphate buffer, pH 7.0, and three times with water for 30 min; 11) staining with 1% uranyl acetate for 10 min; and 12) washing three times with water for 15 min. The grids were retrieved from the mPrep/g capsules, air-dried, and examined in a Tecnai T12 transmission electron microscope (Thermo Fisher) at 80 keV. Images were acquired with an AMT digital camera using AMTV600 software (Advanced Microscopy Techniques).

Statistical analyses

All values were expressed as mean ± S.E. Differences between means were compared using the Student's *t* test or analysis of variance (ANOVA) followed by Tukey's post hoc analysis. Kaplan-Meier survival curves of Pa-infected mice were compared using the Mantel-Cox log-rank test. Statistical significance was defined at $p < 0.05$.

Author contributions—E. L. conceptualization; E. L. and S. E. G. formal analysis; E. L., R. S., A. S. C., S. P. A., and S. E. G. funding acquisition; E. L., W. G., S. W. H., A. L., N. H., R. S., and I. G. L. investigation; E. L., W. G., S. W. H., A. L., N. H., R. S., and I. G. L. methodology; E. L. and S. E. G. writing-original draft; E. L., R. S., A. S. C., S. P. A., and S. E. G. writing-review and editing; R. S., S. P. A., and S. E. G. supervision; H. I. resources.

Acknowledgments—We thank Dr. Alice Prince for supplying PAK/fliC (and PAO1/NanPs) bacteria, Dr. Ru-ching Hsiao for electron microscopy, and Jennifer Davidson for secretarial assistance. This work utilized an electron microscopy sample preparation instrument that was purchased with funding from National Institutes of Health Grant 1S10RR26870–1 and an ASP-1000 mPrep Automatic Specimen Processor (Microscopy Innovations) that was purchased with funding from Department of Defense DURIP Grant 70183-LSRIP.

References

1. Hallstrand, T. S., Hackett, T. L., Altemeier, W. A., Matute-Bello, G., Hansbro, P. M., and Knight, D. A. (2014) Airway epithelial regulation of pulmonary immune homeostasis and inflammation. *Clin. Immunol.* **151,** 1–15 CrossRef Medline
2. Prince, A. (1992) Adhesins and receptors of *Pseudomonas aeruginosa* associated with infection of the respiratory tract. *Microb. Pathog.* **13,** 251–260 CrossRef Medline
3. Ramos, H. C., Rumbo, M., and Sirard, J. C. (2004) Bacterial flagellins: Mediators of pathogenicity and host immune responses in mucosa. *Trends Microbiol.* **12,** 509–517 CrossRef Medline
4. Pier, G. B., and Ramphal, R. (2010) *Pseudomonas aeruginosa.* in *Mandell, Douglas and Bennett's Principles and Practice of Infectious Diseases* (Mandell, G. L., Bennett, J. E., and Dolin, R., eds), pp. 2835–2860, Elsevier/Churchill/Livingstone, Philadelphia, PA
5. Dasgupta, N., Arora, S. K., and Ramphal, R. (2004) The flagellar system of *Pseudomonas aeruginosa.* in *Pseudomonas.* Vol. 1. Genomics, Life Style and Molecular Architecture (Ramos, J.-L., ed), pp. 675–698, Springer, Boston, MA CrossRef
6. Adamo, R., Sokol, S., Soong, G., Gomez, M. I., and Prince, A. (2004) *Pseudomonas aeruginosa* flagella activate airway epithelial cells through asialoGM1 and Toll-like receptor 2 as well as Toll-like receptor 5. *Am. J. Respir. Cell Mol. Biol.* **30,** 627–634 CrossRef Medline
7. Lillehoj, E. P., Kim, B. T., and Kim, K. C. (2002) Identification of *Pseudomonas aeruginosa* flagellin as an adhesin for Muc1 mucin. *Am. J. Physiol. Lung Cell Mol. Physiol.* **282,** L751–L756 CrossRef Medline
8. Lillehoj, E. P., Kim, H., Chun, E. Y., and Kim, K. C. (2004) *Pseudomonas aeruginosa* stimulates phosphorylation of the airway epithelial membrane glycoprotein Muc1 and activates MAP kinase. *Am. J. Physiol. Lung Cell Mol. Physiol.* **287,** L809–L815 CrossRef Medline
9. Hattrup, C. L., and Gendler, S. J. (2008) Structure and function of the cell surface (tethered) mucins. *Annu. Rev. Physiol.* **70,** 431–457 CrossRef Medline
10. Lillehoj, E. P., Kato, K., Lu, W., and Kim, K. C. (2013) Cellular and molecular biology of airway mucins. *Int. Rev. Cell Mol. Biol.* **303,** 139–202 CrossRef Medline
11. Hilkens, J., Ligtenberg, M. J., Vos, H. L., and Litvinov, S. V. (1992) Cell membrane-associated mucins and their adhesion-modulating property. *Trends Biochem. Sci.* **17,** 359–363 CrossRef Medline
12. Müller, S., Alving, K., Peter-Katalinic, J., Zachara, N., Gooley, A. A., and Hanisch, F. G. (1999) High density *O*-glycosylation on tandem repeat peptide from secretory MUC1 of T47D breast cancer cells. *J. Biol. Chem.* **274,** 18165–18172 CrossRef Medline
13. Storr, S. J., Royle, L., Chapman, C. J., Hamid, U. M., Robertson, J. F., Murray, A., Dwek, R. A., and Rudd, P. M. (2008) The *O*-linked glycosylation of secretory/shed MUC1 from an advanced breast cancer patient's serum. *Glycobiology* **18,** 456–462 CrossRef Medline
14. Litvinov, S. V., and Hilkens, J. (1993) The epithelial sialomucin, episialin, is sialylated during recycling. *J. Biol. Chem.* **268,** 21364–21371 Medline
15. Li, Y., Kuwahara, H., Ren, J., Wen, G., and Kufe, D. (2001) The c-Src tyrosine kinase regulates signaling of the human DF3/MUC1 carcinoma-associated antigen with GSK3β and β-catenin. *J. Biol. Chem.* **276,** 6061–6064 CrossRef Medline
16. Li, Y., Ren, J., Yu, W., Li, Q., Kuwahara, H., Yin, L., Carraway, K. L., 3rd, and Kufe, D. (2001) The epidermal growth factor receptor regulates interaction of the human DF3/MUC1 carcinoma antigen with c-Src and β-catenin. *J. Biol. Chem.* **276,** 35239–35242 CrossRef Medline
17. Yamamoto, M., Bharti, A., Li, Y., and Kufe, D. (1997) Interaction of the DF3/MUC1 breast carcinoma-associated antigen and β-catenin in cell adhesion. *J. Biol. Chem.* **272,** 12492–12494 CrossRef Medline
18. Bonten, E., van der Spoel, A., Fornerod, M., Grosveld, G., and d'Azzo, A. (1996) Characterization of human lysosomal neuraminidase defines the molecular basis of the metabolic storage disorder sialidosis. *Genes Dev.* **10,** 3156–3169 CrossRef Medline
19. Lillehoj, E. P., Hyun, S. W., Feng, C., Zhang, L., Liu, A., Guang, W., Nguyen, C., Luzina, I. G., Atamas, S. P., Passaniti, A., Twaddell, W. S., Puché, A. C., Wang, L. X., Cross, A. S., and Goldblum, S. E. (2012) NEU1 sialidase expressed in human airway epithelia regulates epidermal growth factor receptor (EGFR) and MUC1 protein signaling. *J. Biol. Chem.* **287,** 8214–8231 CrossRef Medline
20. Lillehoj, E. P., Hyun, S. W., Liu, A., Guang, W., Verceles, A. C., Luzina, I. G., Atamas, S. P., Kim, K. C., and Goldblum, S. E. (2015) NEU1 sialidase regulates membrane-tethered mucin (MUC1) ectodomain adhesiveness for *Pseudomonas aeruginosa* and decoy receptor release. *J. Biol. Chem.* **290,** 18316–18331 CrossRef Medline
21. Thathiah, A., Blobel, C. P., and Carson, D. D. (2003) Tumor necrosis factor-α converting enzyme/ADAM17 mediates MUC1 shedding. *J. Biol. Chem.* **27,** 3386–3394 CrossRef Medline
22. Julian, J., Dharmaraj, N., and Carson, D. D. (2009) MUC1 is a substrate for γ-secretase. *J. Cell. Biochem.* **108,** 802–815 CrossRef Medline
23. Thathiah, A., and Carson, D. D. (2004) MT1-MMP mediates MUC1 shedding independent of TACE/ADAM17. *Biochem. J.* **382,** 363–373 CrossRef Medline
24. Lindén, S. K., Sheng, Y. H., Every, A. L., Miles, K. M., Skoog, E. C., Florin, T. H., Sutton, P., and McGuckin, M. A. (2009) MUC1 limits *Helicobacter pylori* infection both by steric hindrance and by acting as a releasable decoy. *PLoS Pathog.* **5,** e1000617 CrossRef Medline
25. Allison, J. S., Dawson, M., Drake, D., and Montie, T. C. (1985) Electrophoretic separation and molecular weight characterization of *Pseudomonas aeruginosa* H-antigen flagellins. *Infect. Immun.* **49,** 770–774 Medline
26. Ali, M., Lillehoj, E. P., Park, Y., Kyo, Y., and Kim, K. C. (2011) Analysis of the proteome of human airway epithelial secretions. *Proteome Sci.* **9,** 4 CrossRef Medline
27. Kesimer, M., Kirkham, S., Pickles, R. J., Henderson, A. G., Alexis, N. E., Demaria, G., Knight, D., Thornton, D. J., and Sheehan, J. K. (2009) Tracheobronchial air-liquid interface cell culture: A model for innate mucosal defense of the upper airways? *Am. J. Physiol. Lung Cell Mol. Physiol.* **296,** L92–L100 CrossRef Medline

28. Song, J. A., Yang, H. S., Lee, J., Kwon, S., Jung, K. J., Heo, J. D., Cho, K. H., Song, C. W., and Lee, K. (2010) Standardization of bronchoalveolar lavage method based on suction frequency number and lavage fraction number using rats. *Toxicol. Res.* **26,** 203–208 CrossRef Medline
29. Erhardt, M., Namba, K., and Hughes, K. T. (2010) Bacterial nanomachines: The flagellum and type III injectisome. *Cold Spring Harb. Perspect. Biol.* **2,** a000299 CrossRef Medline
30. Hyun, S. W., Liu, A., Liu, Z., Cross, A. S., Verceles, A. C., Magesh, S., Kommagalla, Y., Kona, C., Ando, H., Luzina, I. G., Atamas, S. P., Piepenbrink, K. H., Sundberg, E. J., Guang, W., Ishida, H., Lillehoj, E. P., and Goldblum, S. E. (2016) The NEU1-selective sialidase inhibitor, C9-butyl-amide-DANA, blocks sialidase activity and NEU1-mediated bioactivities in human lung *in vitro* and murine lung *in vivo*. *Glycobiology* **26,** 834–849 CrossRef Medline
31. Goldblum, S. E., Wu, K. M., and Jay, M. (1985) Lung myeloperoxidase as a measure of pulmonary leukostasis in rabbits. *J. Appl. Physiol.* **59,** 1978–1985 CrossRef Medline
32. Meindl, P., and Tuppy, H. (1969) 2-Deoxy-2,3-dehydrosialic acids. II. Competitive inhibition of *Vibrio cholerae* neuraminidase by 2-deoxy-2,3-dehydro-*N*-acylneuraminic acids. *Hoppe Seylers Z. Physiol. Chem.* **350,** 1088–1092 CrossRef Medline
33. Burmeister, W. P., Henrissat, B., Bosso, C., Cusack, S., and Ruigrok, R. W. (1993) Influenza B virus neuraminidase can synthesize its own inhibitor. *Structure* **1,** 19–26 CrossRef Medline
34. Luzina, I. G., Lockatell, V., Hyun, S. W., Kopach, P., Kang, P. H., Noor, Z., Liu, A., Lillehoj, E. P., Lee, C., Miranda-Ribera, A., Todd, N. W., Goldblum, S. E., and Atamas, S. P. (2016) Elevated expression of NEU1 sialidase in idiopathic pulmonary fibrosis provokes pulmonary collagen deposition, lymphocytosis, and fibrosis. *Am. J. Physiol. Lung Cell Mol. Physiol.* **310,** L940–L954 CrossRef Medline
35. Soong, G., Muir, A., Gomez, M. I., Waks, J., Reddy, B., Planet, P., Singh, P. K., Kanetko, Y., Wolfgang, M. C., Hsiao, Y. S., Tong, L., and Prince, A. (2006) Bacterial neuraminidase facilitates mucosal infection by participating in biofilm production. *J. Clin. Invest.* **116,** 2297–2305 CrossRef Medline
36. Hsiao, Y. S., Parker, D., Ratner, A. J., Prince, A., and Tong, L. (2009) Crystal structures of respiratory pathogen neuraminidases. *Biochem. Biophys. Res. Commun.* **380,** 467–471 CrossRef Medline
37. Lillehoj, E. P., Han, F., and Kim, K. C. (2003) Mutagenesis of a Gly-Ser cleavage site in MUC1 inhibits ectodomain shedding. *Biochem. Biophys. Res. Commun.* **307,** 743–749 CrossRef Medline
38. Vasta, G. R. (2012) Galectins as pattern recognition receptors: Structure, function, and evolution. *Adv. Exp. Med. Biol.* **946,** 21–36 CrossRef Medline
39. Varki, A., Cummings, R. D., and Esko, J. D. (2009) *Essentials of Glycobiology.* 2nd Ed., Cold Spring Harbor Laboratory, Cold Spring Harbor, NY
40. Ramasamy, S., Duraisamy, S., Barbashov, S., Kawano, T., Kharbanda, S., and Kufe, D. (2007) The MUC1 and galectin-3 oncoproteins function in a microRNA-dependent regulatory loop. *Mol. Cell* **27,** 992–1004 CrossRef Medline
41. Mori, Y., Akita, K., Yashiro, M., Sawada, T., Hirakawa, K., Murata, T., and Nakada, H. (2015) Binding of galectin-3, a β-galactoside-binding lectin, to MUC1 protein enhances phosphorylation of extracellular signal-regulated kinase 1/2 (ERK1/2) and Akt, promoting tumor cell malignancy. *J. Biol. Chem.* **290,** 26125–26140 CrossRef Medline
42. Oberg, C. T., Leffler, H., and Nilsson, U. J. (2011) Inhibition of galectins with small molecules. *Chimia* **65,** 18–23 Medline
43. Khow, O., and Suntrarachun, S. (2012) Strategies for production of active eukaryotic proteins in bacterial expression system. *Asian Pac. J. Trop. Biomed.* **2,** 159–162 CrossRef Medline
44. Price, M. R., Rye, P. D., Petrakou, E., Murray, A., Brady, K., Imai, S., Haga, S., Kiyozuka, Y., Schol, D., Meulenbroek, M. F., Snijdewint, F. G., von Mensdorff-Pouilly, S., Verstraeten, R. A., Kenemans, P., Blockzjil, A., *et al.* (1998) Summary report on the ISOBM TD-4 Workshop: Analysis of 56 monoclonal antibodies against the MUC1 mucin. San Diego, CA, November 17–23, 1996. *Tumour Biol.* **19,** Suppl. 1, 1–20 Medline
45. Burchell, J. M., Mungul, A., and Taylor-Papadimitriou, J. (2001) *O*-linked glycosylation in the mammary gland: Changes that occur during malignancy. *J. Mammary Gland Biol. Neoplasia* **6,** 355–364 CrossRef Medline
46. Lacunza, E., Bara, J., Segal-Eiras, A., and Croce, M. V. (2009) Expression of conserved mucin domains by epithelial tissues in various mammalian species. *Res. Vet. Sci.* **86,** 68–77 CrossRef Medline
47. Totten, P. A., and Lory, S. (1990) Characterization of the type a flagellin gene from *Pseudomonas aeruginosa* PAK. *J. Bacteriol.* **172,** 7188–7199 CrossRef Medline
48. Stover, C. K., Pham, X. Q., Erwin, A. L., Mizoguchi, S. D., Warrener, P., Hickey, M. J., Brinkman, F. S., Hufnagle, W. O., Kowalik, D. J., Lagrou, M., Garber, R. L., Goltry, L., Tolentino, E., Westbrock-Wadman, S., Yuan, Y., *et al.* (2000) Complete genome sequence of *Pseudomonas aeruginosa* PAO1, an opportunistic pathogen. *Nature* **406,** 959–964 CrossRef Medline
49. Zelová, H., and Hošek, J. (2013) TNF-α signalling and inflammation: Interactions between old acquaintances. *Inflamm. Res.* **62,** 641–651 CrossRef Medline
50. Zachariae, C. O. (1993) Chemotactic cytokines and inflammation. Biological properties of the lymphocyte and monocyte chemotactic factors ELCF, MCAF and IL-8. *Acta Derm. Venereol. Suppl.* **181,** 1–37 Medline
51. Kim, K. C., Wasano, K., Niles, R. M., Schuster, J. E., Stone, P. J., and Brody, J. S. (1987) Human neutrophil elastase releases cell surface mucins from primary cultures of hamster tracheal epithelial cells. *Proc. Natl. Acad. Sci. U.S.A.* **84,** 9304–9308 CrossRef Medline
52. Lillehoj, E. P., Hyun, S. W., Kim, B. T., Zhang, X. G., Lee, D. I., Rowland, S., and Kim, K. C. (2001) Muc1 mucins on the cell surface are adhesion sites for *Pseudomonas aeruginosa*. *Am. J. Physiol. Lung Cell Mol. Physiol.* **280,** L181–L187 CrossRef Medline
53. Champigny, M. J., Johnson, M., and Igdoura, S. A. (2003) Characterization of the mouse lysosomal sialidase promoter. *Gene* **319,** 177–187 CrossRef Medline
54. Lukong, K. E., Seyrantepe, V., Landry, K., Trudel, S., Ahmad, A., Gahl, W. A., Lefrancois, S., Morales, C. R., and Pshezhetsky, A. V. (2001) Intracellular distribution of lysosomal sialidase is controlled by the internalization signal in its cytoplasmic tail. *J. Biol. Chem.* **276,** 46172–46181 CrossRef Medline
55. Liang, F., Seyrantepe, V., Landry, K., Ahmad, R., Ahmad, A., Stamatos, N. M., and Pshezhetsky, A. V. (2006) Monocyte differentiation up-regulates the expression of the lysosomal sialidase, Neu1, and triggers its targeting to the plasma membrane via major histocompatibility complex class II-positive compartments. *J. Biol. Chem.* **281,** 27526–27538 CrossRef Medline
56. Nan, X., Carubelli, I., and Stamatos, N. M. (2007) Sialidase expression in activated human T lymphocytes influences production of IFN-γ. *J. Leukoc. Biol.* **81,** 284–296 CrossRef Medline
57. Cross, A. S., Hyun, S. W., Miranda-Ribera, A., Feng, C., Liu, A., Nguyen, C., Zhang, L., Luzina, I. G., Atamas, S. P., Twaddell, W. S., Guang, W., Lillehoj, E. P., Puché, A. C., Huang, W., Wang, L. X., Passaniti, A., and Goldblum, S. E. (2012) NEU1 and NEU3 sialidase activity expressed in human lung microvascular endothelia: NEU1 restrains endothelial cell migration, whereas NEU3 does not. *J. Biol. Chem.* **287,** 15966–15980 CrossRef Medline
58. D'Avila, F., Tringali, C., Papini, N., Anastasia, L., Croci, G., Massaccesi, L., Monti, E., Tettamanti, G., and Venerando, B. (2013) Identification of lysosomal sialidase NEU1 and plasma membrane sialidase NEU3 in human erythrocytes. *J. Cell Biochem.* **114,** 204–211 CrossRef Medline
59. Lee, C., Liu, A., Miranda-Ribera, A., Hyun, S. W., Lillehoj, E. P., Cross, A. S., Passaniti, A., Grimm, P. R., Kim, B. Y., Welling, P. A., Madri, J. A., DeLisser, H. M., and Goldblum, S. E. (2014) NEU1 sialidase regulates the sialylation state of CD31 and disrupts CD31-driven capillary-like tube formation in human lung microvascular endothelia. *J. Biol. Chem.* **289,** 9121–9135 CrossRef Medline
60. Amith, S. R., Jayanth, P., Franchuk, S., Finlay, T., Seyrantepe, V., Beyaert, R., Pshezhetsky, A. V., and Szewczuk, M. R. (2010) Neu1 desialylation of sialyl α-2,3-linked β-galactosyl residues of TOLL-like receptor 4 is essential for receptor activation and cellular signaling. *Cell Signal.* **22,** 314–324 CrossRef Medline

61. Duca, L., Blanchevoye, C., Cantarelli, B., Ghoneim, C., Dedieu, S., Delacoux, F., Hornebeck, W., Hinek, A., Martiny, L., and Debelle, L. (2007) The elastin receptor complex transduces signals through the catalytic activity of its Neu-1 subunit. *J. Biol. Chem.* **282,** 12484–12491 CrossRef Medline
62. Hinek, A., Bodnaruk, T. D., Bunda, S., Wang, Y., and Liu, K. (2008) Neuraminidase-1, a subunit of the cell surface elastin receptor, desialylates and functionally inactivates adjacent receptors interacting with the mitogenic growth factors PDGF-BB and IGF-2. *Am. J. Pathol.* **173,** 1042–1056 CrossRef Medline
63. Arabkhari, M., Bunda, S., Wang, Y., Wang, A., Pshezhetsky, A. V., and Hinek, A. (2010) Desialylation of insulin receptors and IGF-1 receptors by neuraminidase-1 controls the net proliferative response of L6 myoblasts to insulin. *Glycobiology* **20,** 603–616 CrossRef Medline
64. Pshezhetsky, A. V., and Ashmarina, L. I. (2013) Desialylation of surface receptors as a new dimension in cell signaling. *Biochemistry* **78,** 736–745 CrossRef Medline
65. Yogalingam, G., Bonten, E. J., van de Vlekkert, D., Hu, H., Moshiach, S., Connell, S. A., and d'Azzo, A. (2008) Neuraminidase 1 is a negative regulator of lysosomal exocytosis. *Dev. Cell* **15,** 74–86 CrossRef Medline
66. Sumida, M., Hane, M., Yabe, U., Shimoda, Y., Pearce, O. M., Kiso, M., Miyagi, T., Sawada, M., Varki, A., Kitajima, K., and Sato, C. (2015) Rapid trimming of cell surface polysialic acid (polySia) by exovesicular sialidase triggers release of preexisting surface neurotrophin. *J. Biol. Chem.* **290,** 13202–13214 CrossRef Medline
67. Maurice, P., Baud, S., Bocharova, O. V., Bocharov, E. V., Kuznetsov, A. S., Kawecki, C., Bocquet, O., Romier, B., Gorisse, L., Ghirardi, M., Duca, L., Blaise, S., Martiny, L., Dauchez, M., Efremov, R. G., and Debelle, L. (2016) New insights into molecular organization of human neuraminidase-1: Transmembrane topology and dimerization ability. *Sci. Rep.* **6,** 38363 CrossRef Medline
68. Plotkowski, M. C., Bajolet-Laudinat, O., and Puchelle, E. (1993) Cellular and molecular mechanisms of bacterial adhesion to respiratory mucosa. *Eur. Respir. J.* **6,** 903–916 Medline
69. Tsang, K. W., Rutman, A., Tanaka, E., Lund, V., Dewar, A., Cole, P. J., and Wilson, R. (1994) Interaction of *Pseudomonas aeruginosa* with human respiratory mucosa *in vitro*. *Eur. Respir. J.* **7,** 1746–1753 CrossRef Medline
70. Chmiel, J. F., and Davis, P. B. (2003) State of the art: Why do the lungs of patients with cystic fibrosis become infected and why can't they clear the infection? *Respir. Res.* **4,** 8 CrossRef Medline
71. Shanks, K. K., Guang, W., Kim, K. C., and Lillehoj, E. P. (2010) Interleukin-8 production by human airway epithelial cells in response to *Pseudomonas aeruginosa* clinical isolates expressing type a or type b flagellins. *Clin. Vaccine Immunol.* **17,** 1196–1202 CrossRef Medline
72. Lu, W., Hisatsune, A., Koga, T., Kato, K., Kuwahara, I., Lillehoj, E. P., Chen, W., Cross, A. S., Gendler, S. J., Gewirtz, A. T., and Kim, K. C. (2006) Cutting edge: Enhanced pulmonary clearance of *Pseudomonas aeruginosa* by Muc1 knockout mice. *J. Immunol.* **176,** 3890–3894 CrossRef Medline
73. Pollack, M. (1984) The virulence of *Pseudomonas aeruginosa*. *Rev. Infect. Dis.* **6,** Suppl. 3, S617–S626 Medline
74. Luzar, M. A., Thomassen, M. J., and Montie, T. C. (1985) Flagella and motility alterations in *Pseudomonas aeruginosa* strains from patients with cystic fibrosis: Relationship to patient clinical condition. *Infect. Immun.* **50,** 577–582 Medline
75. Mahenthiralingam, E., Campbell, M. E., and Speert, D. P. (1994) Nonmotility and phagocytic resistance of *Pseudomonas aeruginosa* isolates from chronically colonized patients with cystic fibrosis. *Infect. Immun.* **62,** 596–605 Medline
76. Wolfgang, M. C., Jyot, J., Goodman, A. L., Ramphal, R., and Lory, S. (2004) *Pseudomonas aeruginosa* regulates flagellin expression as part of a global response to airway fluid from cystic fibrosis patients. *Proc. Natl. Acad. Sci. U.S.A.* **101,** 6664–6668 CrossRef Medline
77. Palmer, K. L., Mashburn, L. M., Singh, P. K., and Whiteley, M. (2005) Cystic fibrosis sputum supports growth and cues key aspects of *Pseudomonas aeruginosa* physiology. *J. Bacteriol.* **187,** 5267–5277 CrossRef Medline
78. Magesh, S., Moriya, S., Suzuki, T., Miyagi, T., Ishida, H., and Kiso, M. (2008) Design, synthesis, and biological evaluation of human sialidase inhibitors. Part 1: Selective inhibitors of lysosomal sialidase (NEU1). *Bioorg. Med. Chem. Lett.* **18,** 532–537 CrossRef Medline
79. Simon, R., Curtis, B., Deumic, V., Nicki, J., Tennant, S. M., Pasetti, M. F., Lees, A., Wills, P. W., Chacon, M., and Levine, M. M. (2014) A scalable method for biochemical purification of *Salmonella* flagellin. *Protein Expr. Purif.* **102,** 1–7 CrossRef Medline
80. Hegerle, N., Choi, M., Sinclair, J., Amin, M. N., Ollivault-Shiflett, M., Curtis, B., Laufer, R. S., Shridhar, S., Brammer, J., Toapanta, F. R., Holder, I. A., Pasetti, M. F., Lees, A., Tennant, S. M., Cross, A. S., and Simon, R. (2018) Development of a broad spectrum glycoconjugate vaccine to prevent wound and disseminated infections with *Klebsiella pneumoniae* and *Pseudomonas aeruginosa*. *PLoS One* **13,** e0203143 CrossRef Medline

Neuraminidase 1–mediated desialylation of the mucin 1 ectodomain releases a decoy receptor that protects against *Pseudomonas aeruginosa* lung infection

Erik P. Lillehoj, Wei Guang, Sang W. Hyun, Anguo Liu, Nicolas Hegerle, Raphael Simon, Alan S. Cross, Hideharu Ishida, Irina G. Luzina, Sergei P. Atamas and Simeon E. Goldblum

J. Biol. Chem. 2019, 294:662-678.
doi: 10.1074/jbc.RA118.006022 originally published online November 14, 2018